Taylor & Francis
Taylor & Francis Group

BASIC RESEARCH PAPER

🔓 OPEN ACCESS

Ubiquitination of ERMES components by the E3 ligase Rsp5 is involved in mitophagy

Naïma Belgareh-Touzé, Laetitia Cavellini, and Mickael M. Cohen

UMR8226, CNRS/UPMC, Sorbonne Université, Institut de Biologie Physico-Chimique, Paris, France

ABSTRACT

Mitochondria are dynamic organelles that undergo permanent fission and fusion events. These processes play an essential role in maintaining normal cellular function. In the yeast *Saccharomyces cerevisiae*, the endoplasmic reticulum-mitochondrial encounter structure (ERMES) is a marker of sites of mitochondrial division, but it is also involved in a plethora of other mitochondrial functions. However, it remains unclear how these different functions are regulated. We show here that Mdm34 and Mdm12, 2 components of ERMES, are ubiquitinated by the E3 ligase Rsp5. This ubiquitination is not involved in mitochondrial dynamics or in the distribution and turnover of ERMES. Nevertheless, the ubiquitination of Mdm34 and Mdm12 was required for efficient mitophagy. We thus report here the first identification of ubiquitinated substrates participating in yeast mitophagy.

Introduction

Mitochondria are double-membrane-bound organelles organized into dynamic tubular networks with a morphology conditioned by the balance between mitochondrial membrane fusion and fission.[1,2] The predominance of one of these events over the other results in hyperfused or highly fragmented mitochondria, with effects on all mitochondrial functions, from oxidative phosphorylation to lipid metabolism, calcium homeostasis, cell signaling and organelle quality control.[2,3]

The fusion and fission of mitochondrial membranes need large GTPases of the dynamin-related proteins (DRPs) family. MFNs (mitofusins) and OPA1 (Mgm1 in yeast) are transmembrane DRPs that promote the anchoring and fusion of the mitochondrial outer and inner membranes, respectively. Fission requires a cytosolic DRP (Dnm1 in yeast; DNM1L in metazoans) that is recruited to the outer membrane and mediates constriction followed by mitochondrial tubule separation. The sites of DRP recruitment are not random; instead, they correspond to regions in which the endoplasmic reticulum wraps around mitochondrial tubules.[4] This process, known as ER-associated mitochondrial division (ERMD), has been characterized thoroughly in yeast and involves the multiprotein ER-mitochondrial encounter structure (ERMES).

The ERMES complex consists of the mitochondrial outer membrane proteins Mdm10 and Mdm34, the ER integral membrane protein Mmm1 and the cytosolic protein Mdm12, which serves as a bridge between the ER and the mitochondria.[5] ERMES tethers the mitochondria to the ER and acts as a marker of sites of mitochondrial division, together with

Gem1, a rho-like GTPase of the outer membrane that acts as a regulatory subunit of ERMES.[6,7] At these sites, the complex is colocalized with replicating mitochondrial DNA (mtDNA), providing a connection between the division of mitochondria and the distribution of mtDNA.[8-10] Following division, the distribution of ERMES is asymmetric, with this complex associated with only one of the 2 mitochondrial tips.

ERMES function is not restricted to ERMD. The ERMES component Mdm10 is a β-barrel protein, that also belongs to the SAM (sorting and assembly machinery) complex, implicated in the insertion of ß-barrel proteins into the mitochondrial outer membrane.[11] Mitochondrial division at the ER is required for the selective degradation of mitochondria by autophagy, and ERMES is implicated in this mitophagy-specific fission process.[12-14] It has also been suggested that ERMES supplies the growing autophagosome with lipids during mitophagy. Consistent with this possibility, Mdm34, Mmm1 and Mdm12 contain SMP (synaptotagmin-like, mitochondrial and lipid-binding proteins) domains that probably mediate the exchange of lipids between the ER and the mitochondria.[15-17] On the basis of its interaction with the peroxisomal protein Pex11, Mdm34 has also been implicated in the establishment of physical contact between mitochondria and peroxisomes, a process independent of Mmm1 and Gem1.[18,19] ERMES components may therefore be involved in transferring lipids to mitochondria from other organelles.

Mutants lacking any of the ERMES components have giant swollen mitochondria, lack mtDNA nucleoids and cannot grow on a respiratory medium. These defects reflect the diversity of

ERMES functions in the regulation of mitochondrial homeostasis. However, the molecular principles underlying the role of the complex in mitochondrial fission, mtDNA distribution, mitophagy or lipid transit between organelles are unknown. Mdm34 undergoes ubiquitination;[20] this modification may separate out the different functions of ERMES components, but its precise role in this content remains to be determined.

Ubiquitination is the formation of a covalent bond between the C-terminal end of ubiquitin (a 76-amino acid polypeptide) and the amino side group of a lysine residue within a target protein referred to as the "substrate."[21] Ubiquitin contains 7 lysine residues and can itself be ubiquitinated, giving rise to poly-ubiquitin chains. The lysine residue of ubiquitin used to link ubiquitin moieties defines the function of the ubiquitin chains. For instance, lysine 48-linked ubiquitin chains (UbK48) are the main signal for targeting to a multimeric degradation complex called the proteasome. By contrast, UbK63 chains or the modification of substrates with single ubiquitin moieties may mediate regulatory functions that are mostly independent of substrate targeting to the proteasome.[21] The type of bonding to ubiquitin depends on the ubiquitin-conjugating enzymes (E2s) and ubiquitin ligases (E3s) involved. E3s determine the substrate specificity of ubiquitination by binding to both substrates and E2s. There are 3 major categories of E3s, defined on the basis of the mode of ubiquitin transfer from the E2 to the substrate: RING (really interesting new genes), HECT (homologous to E6-associated protein C terminus) catalytic domain or RBR (RING between RINGs) enzymes.[22,23] RING E3s mediate the direct transfer of ubiquitin from the E2 to the substrate. HECT E3s differ from RINGs in that they accept ubiquitin from E2s on a conserved cysteine of the HECT domain and then transfer the ubiquitin to the target substrate. RBR E3s contain a first RING domain that binds to E2s. However, like HECT E3s, they catalyze the transfer of ubiquitin from the E2 to the catalytic cysteine of a second RING domain before its transfer to the substrate.[23]

Members of each of these E3 groups have been shown to be essential for the regulation of mitochondrial homeostasis. In yeast, the HECT E3 Rsp5 was the first ubiquitin ligase shown to regulate mitochondrial function and inheritance.[24,25] The SCF-Mdm30 (Skp1/Cullin/F-box protein with Mdm30 as the F-box protein) complex is a multimeric RING E3 that promotes K48-ubiquitination and subsequent proteasomal degradation of the yeast mitofusin Fzo1.[26,27] In addition to this established role in the regulation of mitochondrial fusion, the SCF-Mdm30 has also been shown to be responsible for ubiquitination of the Mdm34 ERMES component.[20] PARK2/Parkin is an RBR E3 that has been implicated in the onset of juvenile Parkinson disease and plays a crucial role in mitophagy.[28]

Mitophagy involves integral proteins of the mitochondrial outer membrane containing Atg8-interacting motifs (AIMs, referred to as LC3-interacting regions [LIRs] in more complex eukaryotes) in their cytosolic domains. These AIMs/LIRs bind Atg8/LC3-family proteins, thereby recruiting the autophagic machinery.[29] In yeast, this pathway requires the AIM-containing Atg32 receptor.[30] Following the induction of mitophagy, Atg32 is phosphorylated and recruits the soluble factor Atg11, before interacting with Atg8.[30,31] In mammalian cells, there is an additional ubiquitin-dependent mitophagy pathway that is

dependent on the RBR E3 ligase PARK2/Parkin.[32] PARK2 is selectively recruited to depolarized mitochondria, where it induces the ubiquitination of outer membrane substrates.[33] The subsequent recruitment of receptors with ubiquitin-binding domains and LIR motifs triggers the degradation of ubiquitin-tagged mitochondria by autophagy. Clues to the role of ubiquitin in yeast mitophagy have recently been obtained.[34] However, the E3 ligase and the ubiquitination substrates involved in this process remain to be identified.

We show here that Mdm34 ubiquitination is dependent on Rsp5. We also show that this HECT E3 promotes the ubiquitination of Mdm12. Ubiquitin-dependent modification of these 2 ERMES components did not affect ERMD, the distribution of mtDNA or the localization of ERMES to sites of contact between the ER and mitochondria. However, the Rsp5-mediated regulation of ERMES was found to be required for efficient mitophagy.

Results

Mdm34 is a substrate of Rsp5

We investigated the role of Mdm34 ubiquitination by the ubiquitin ligase SCF-Mdm30, by generating "wild-type" (for *MDM30*) and *mdm30Δ* strains in which the C-terminal part of *MDM34* was fused to 9 MYC epitopes, at the chromosomal locus. The resulting wild-type strain displayed no growth defect on YPD or YPG, demonstrating that the tagged version of *MDM34* was functional (Fig. S1A). Yeast crude protein extracts from wild-type and *mdm30Δ* strains grown to mid-exponential growth phase were separated by SDS-PAGE and analyzed by western blotting with a monoclonal anti-MYC antibody. In these conditions, slowly migrating species potentially corresponding to ubiquitinated Mdm34 were barely visible (Fig. 1A, upper panel, lane ø). We then overproduced untagged or 6-HIS-tagged ubiquitin, to optimize the detection of Mdm34 ubiquitination.

Upon ubiquitin overexpression, confirmed by immunoblotting with an anti-ubiquitin antibody (Fig. 1A lower panel), we were able to detect at least 3 slowly migrating Mdm34 bands in the wild-type strain (Fig. 1A and Fig. S1B). These species corresponded to ubiquitinated Mdm34, because a shift in molecular weight was observed when the overproduced ubiquitin was tagged with histidine (Fig. 1A and Fig. S1B). Surprisingly, Mdm34 was as ubiquitinated in the *mdm30Δ* strain as in the wild-type strain indicating that, upon ubiquitin overexpression, the SCF-Mdm30 ubiquitin ligase is not involved in Mdm34 ubiquitination (Fig. 1A).

Two studies have identified Mdm34 as one of the binding partners of the Rsp5 ubiquitin ligase.[35,36] We therefore assessed the possible role of Rsp5 in the ubiquitination of Mdm34. The deletion of *RSP5* is lethal and its essential function is the induction of ubiquitin proteasome-dependent processing and activation of the transcription factor Spt23, which promotes the synthesis of the Δ9 fatty acid desaturase enzyme Ole1.[37] We produced C-terminally tagged Mdm34 in an *rsp5Δ* strain complemented with the truncated version of Spt23 (hereafter called *rsp5Δ* p*spt23ΔCT*). In the absence of Rsp5, Mdm34 ubiquitination, upon ubiquitin overexpression, was completely abolished (Fig. 1A).
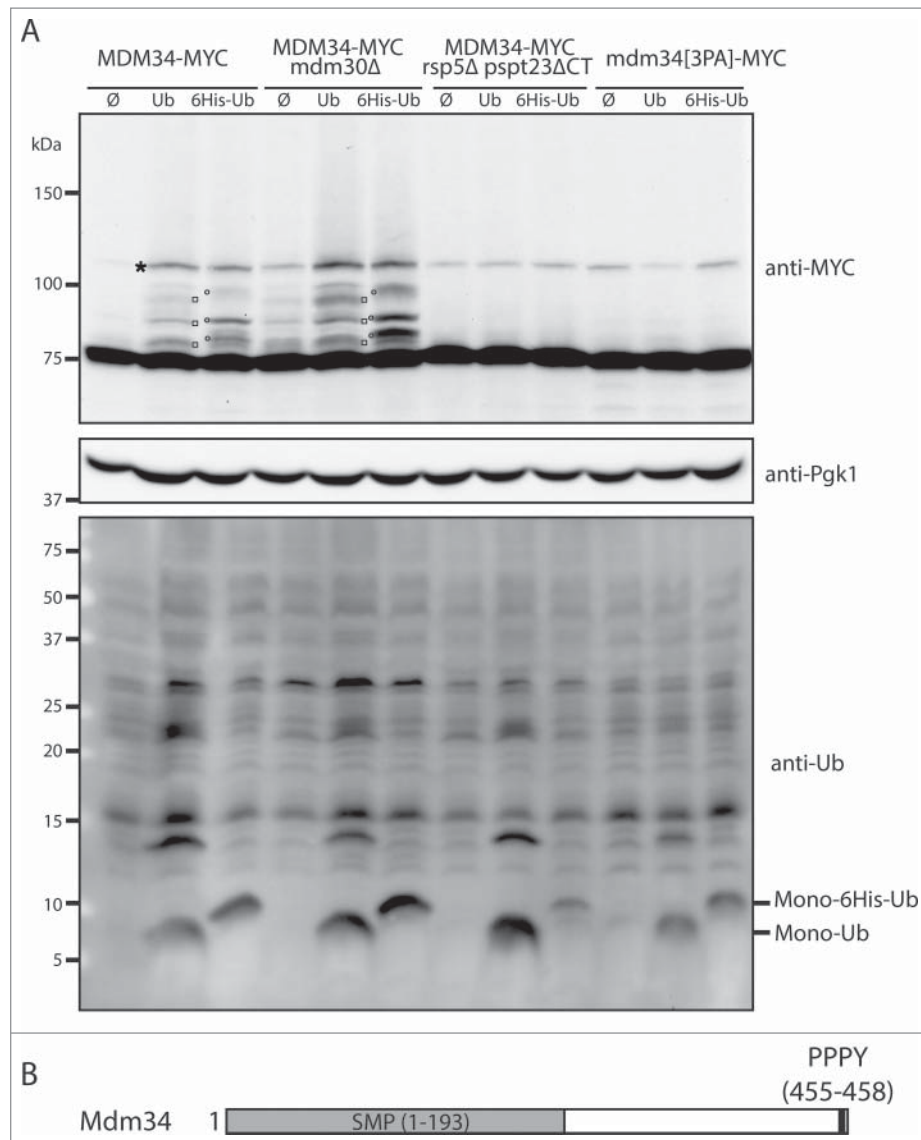
Figure 1. Mdm34 is directly ubiquitinated by Rsp5. (A) *MDM34-MYC, MDM34-MYC mdm30Δ, MDM34-MYC rsp5Δ pspt23ΔCT* and *mdm34[3PA]-MYC* strains transformed with plasmids expressing ubiquitin (Ub), ubiquitin tagged with 6-histidines (6His-Ub) or with an empty plasmid (Ø) were grown at 30°C in YNB with glucose as the carbon source. Copper (CuSO4, 100 μM) was added to the cell cultures for 1 h to induce ubiquitin synthesis from the *CUP1* promoter. Total protein extracts were prepared and analyzed by western immunoblotting with antibodies directed against MYC (anti-MYC), ubiquitin (anti-Ub), or phosphoglycerate kinase (anti-Pgk1) as a loading control. Monoubiquitin (Mono-Ub) and monoubiquitin tagged with 6 histidine residues (Mono-6His-Ub) are indicated. □, Mdm34-MYC conjugated with ubiquitin; ', Mdm34-MYC conjugated with 6His-ubiquitin; *, Nonspecific band. (B) Schematic representation of Mdm34. The PPPY motif is shown in black and the SMP domains (synaptotagmin-like, mitochondrial and lipid-binding proteins) in gray.

We inhibited the presumed interaction between the 2 proteins, to confirm the direct requirement for Rsp5 in Mdm34 ubiquitination. Rsp5 belongs to the NEDD4 (neural precursor cell-expressed, developmentally downregulated) family of HECT E3s. These proteins share similar domain architectures, with an N-terminal C2 domain that binds membrane phosphoinositides, 2–4 WW (Trp-Trp) protein-protein interaction modules, and a C-terminal HECT domain. Rsp5 contains 3 WW domains that bind short recognition sequences ([L/P] PXY) called PY motifs.[22,38,39] Mdm34 has a PPPY sequence at its C terminus and interacts with the WW3 domain of Rsp5[35] or with the full-length ubiquitin ligase.[36] The Mdm34 PY motif is located only one amino acid upstream from the stop codon (Fig. 1B). We were therefore able to mutate the PY motif directly at the chromosomal locus (PPPY→AAAY) to generate the *mdm34[3PA]-MYC* strain. This mutation did not affect the

viability of the strain (Fig. S1A) but resulted in an almost total absence of Mdm34 ubiquitination (Fig. 1A and Fig. S1B). Thus, in conditions of ubiquitin overproduction, Mdm34 is a substrate for Rsp5-mediated ubiquitination.

Mdm12 is also a substrate of Rsp5

The PY motif in Mdm34 probably recruits Rsp5, triggering the ubiquitination of Mdm34. However, Mdm34 is part of the ERMES complex and the proximity of Rsp5 may lead to the ubiquitination of partner proteins interacting with Mdm34. We checked whether the other ERMES components were subject to Rsp5-mediated ubiquitination. We first confirmed the functionality of the *MDM12, MMM1, MDM10* and *GEM1* genes tagged with 9*MYC* epitopes (Fig. S2A), and then analyzed the migration profiles of all ERMES components in conditions of
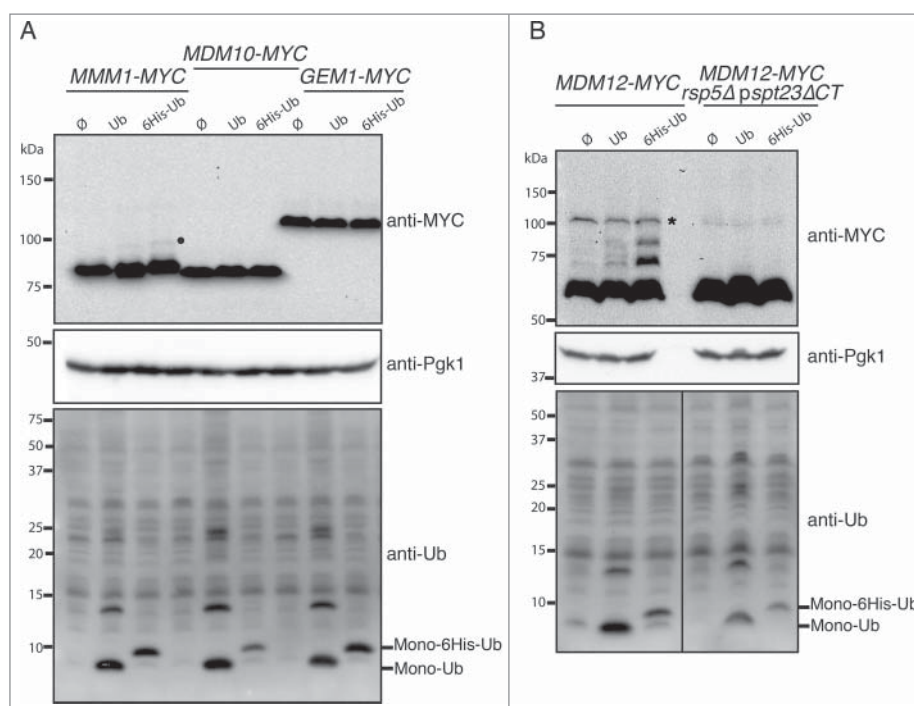
Figure 2. Mdm12 is a new target of Rsp5 ubiquitination. (A, B) The *MMM1-MYC, MDM10-MYC, GEM1-MYC* (A) *MDM12-MYC*, and *MDM12-MYC rsp5Δ* p*spt23ΔCT* (B) strains bearing plasmids encoding ubiquitin (Ub), ubiquitin tagged with 6 histidines (6His-Ub) or an empty plasmid (Ø) were grown at 30°C in YNB supplemented with glucose. CuSO4 (100 μM) was added to the cell cultures for 1 h to induce ubiquitin synthesis from the *CUP1* promoter. Total protein extracts were prepared and analyzed by western immunoblotting with anti-MYC (anti-MYC), anti-ubiquitin (anti-Ub) and anti-phosphoglycerate kinase (anti-Pgk1) antibodies. Pgk1 was used as a loading control. ●, Glycosylated forms; *, nonspecific band.

ubiquitin overproduction. A few, very faint, slowly migrating species were detected for Mmm1 and Gem1, but not for Mdm10 (Fig. 2A). The slowly migrating bands detected for Gem1 did not correspond to ubiquitin species because they were present in the presence and absence of ubiquitin overproduction. They probably corresponded to another post-translational modification or nonspecific bands. Mmm1 is an N-glycosylated ER membrane protein and the slowly migrating species detected corresponded to glycosylated forms of Mmm1 that disappeared after EndoH$_f$ treatment (Fig. S2B). By contrast, Mdm12 displayed a clear pattern of ubiquitination in the presence, but not in the absence of Rsp5 (Fig. 2B). Thus, Mdm34 and Mdm12 are ubiquitinated by Rsp5, but they do not seem to act as adaptors for the ubiquitination of the other ERMES components in the conditions used.

Mdm34 and Mdm12 are ubiquitinated under fission-inducing conditions

We investigated whether the ERMES components were ubiquitinated under specific physiological conditions. Given that Rsp5 is involved in regulating membrane dynamics and ERMES is a marker of mitochondrial fission,[10] we decided to monitor the ubiquitination of Mdm34 and Mdm12 upon the induction of fission. Consistent with previous observations,[40] cell cycle arrest in the G$_1$ phase, through the treatment of wild-type cells with α factor, induced extensive fragmentation of the mitochondrial networks (Fig. 3A). We then investigated the behavior of ERMES components after α factor treatment in wild-type and *rsp5Δ* p*spt23ΔCT* cells. After 2 h of α factor treatment, faint bands, corresponding to ubiquitinated

proteins, appeared in the *MDM34-MYC* strain (Fig. 3B). These bands were stronger after 4 h of treatment. Ubiquitinated species of Mdm12-MYC were also detected after 4 h of treatment with α factor (Fig. 3B). This ubiquitination was strictly dependent on Rsp5, as no slowly migrating Mdm34 and Mdm12 species were detected in the absence of Rsp5 (Fig. 3B). Furthermore, no ubiquitinated Mdm34 species were detected when the *MDM34* PY motif was mutated (Fig. S3).

Consistent with the results obtained in conditions of ubiquitin overproduction, Mmm1-MYC, Gem1-MYC and Mdm10-MYC were unaffected by α factor treatment in the wild-type and *rsp5*-deleted strains (Fig. S3). We checked that the ubiquitination of Mdm34 and Mdm12 after α factor treatment was associated with the induction of mitochondrial fragmentation rather than cell cycle arrest, by monitoring the ubiquitination pattern of ERMES components under other conditions promoting mitochondrial fission in glucose-containing medium (fermentation) and in glycerol-containing medium (respiration). We optimized the detection of ubiquitinated species of Mdm34 and Mdm12 by tagging *MDM34* and *MDM12* with 13-*MYC* rather than 9-*MYC* (Fig. 3D). The corresponding constructs were *MDM34-13MYC* and *MDM12-13MYC*. Ubiquitination was analyzed during the early (EE) and late exponential (LE) growth phases. Heat shock at 37°C and oxidative stress with H$_2$O$_2$ were used to induce fragmentation of the mitochondrial networks (Fig. 3C). These treatments promoted the PY motif-dependent ubiquitination of Mdm34-13MYC and the ubiquitination of Mdm12-13MYC (Fig. 3D) in both fermentative and respiratory media. These observations are consistent with the correlation between mitochondrial fission and ERMES ubiquitination.
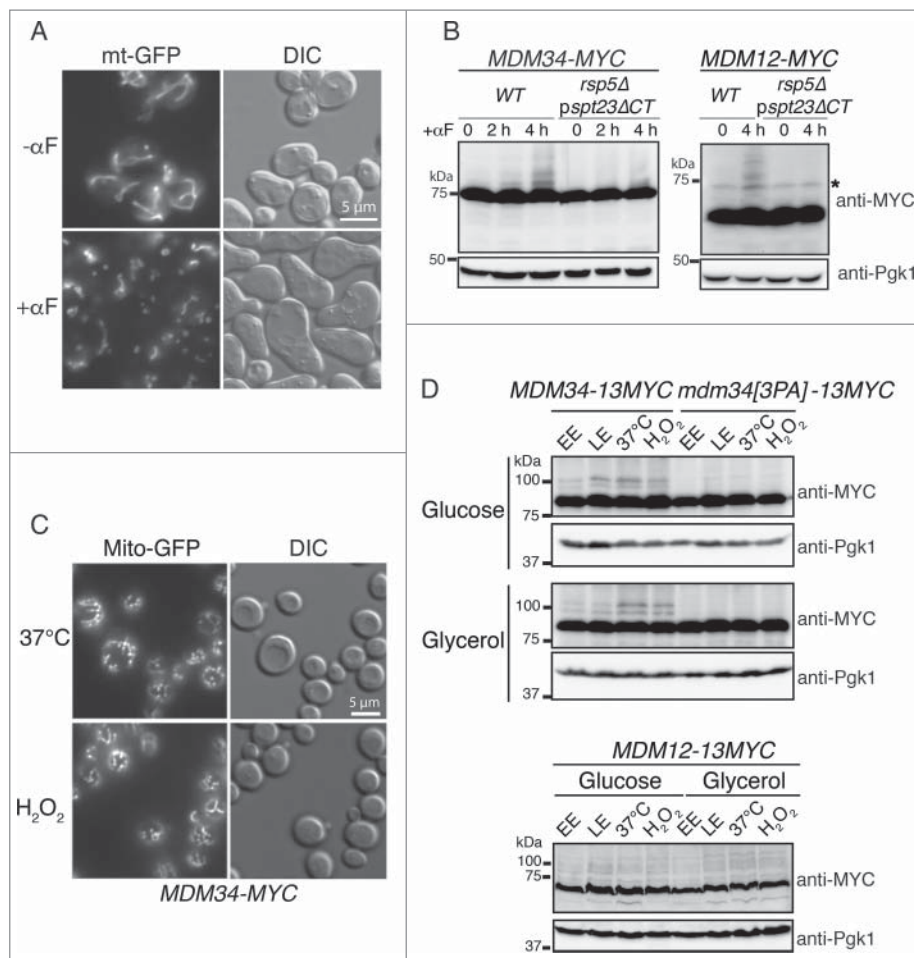
Figure 3. Fission induction promotes the ubiquitination of Mdm34 and Mdm12. (A) Wild-type cells transformed with pYX142-mt-GFP and grown to early exponential growth phase were incubated in the presence (+αF) or absence (−αF) of 50 μg/mL α factor. Live cells were examined with differential interference contrast (DIC) and for GFP fluorescence under a Zeiss microscope. (B) *MDM34-MYC, MDM34-MYC rsp5Δ pspt23ΔCT, MDM12-MYC, MDM12-MYC rsp5Δ pspt23ΔCT* cells were grown to early exponential growth phase in YPD. We added 50 μg/mL α factor (αF) to the medium and total protein extracts were prepared at the times indicated. Proteins were analyzed by western immunoblotting with anti-MYC and anti-phosphoglycerate kinase (anti-Pgk1) antibodies. Pgk1 was used as a loading control. *, nonspecific band. (C) The *MDM34-MYC* strain expressing Mito-GFP from a vector integrated into the chromosome was grown at 30°C in YPD to mid-exponential growth phase. It was then shifted to 37°C or stressed by incubation with 2 mM H_2O_2 for 2 h. Fluorescence microscopy confirmed the presence of fragmented mitochondria after treatment. (D) The *MDM34-13MYC, mdm34[3PA]-13MYC* and *MDM12-13MYC* strains were grown to early exponential phase (EE), late exponential phase (LE), heated at 37°C (37°C) or incubated at 30°C in the presence of 2 mM H_2O_2 (H_2O_2) for 2 h, in medium containing glucose (YPD) or glycerol (YPG). Total protein extracts were prepared and subjected to western immunoblotting with antibodies against MYC (anti-MYC) and phosphoglycerate kinase (anti-Pgk1) as a loading control.

Having determined the conditions in which the Rsp5-dependent ubiquitination of Mdm34 and Mdm12 occurred, we investigated the possible connections between the modifications of these 2 components. We analyzed Mdm12 expression upon heat shock in wild-type and *mdm34[3PA]* strains (Fig. 4A). The ubiquitination of Mdm12-13MYC was efficiently detected after 30 min of incubation at 37°C and remained present over a 2-h period of heat shock in the wild-type strain. By contrast, mutation of the PY motif of Mdm34 resulted in much lower levels of Mdm12-13MYC ubiquitination (Fig. 4A). Thus, the mutation of a single PY motif in the ERMES complex abolished the ubiquitination of both targets of Rsp5: Mdm34 and Mdm12.

An analysis of the peptide sequences of Mdm12 and Mmm1 revealed the presence of 2 putative L/PPXY motifs at the N terminus of Mdm12 (LPSY) and in the central region of Mmm1 (LPEY) facing the cytosol. It was unclear whether all these PY motifs were involved in the interaction with Rsp5, forming a recruitment platform for the ligase, or whether the PY motif of

Mdm34 was the only motif required for the ubiquitination of Mdm34 and Mdm12. We tested this second hypothesis, by constructing a plasmid encoding Mdm12 tagged with 13MYC, either wild-type or with a mutation of the PY motif (LPSY→AAAY). The resulting plasmids were introduced into a strain with an *mdm12* deletion, and ubiquitination was analyzed in the late exponential growth phase. The ubiquitination pattern of Mdm12[3A]-13MYC was compared with that of the strain bearing the chromosomally encoded Mdm12-13MYC (Fig. 4B). The ubiquitination pattern of Mdm12 was not affected by the mutation of its PY motif. The ubiquitination of Mdm34 and Mdm12 was, therefore, strictly dependent on the PY motif of Mdm34.

Analysis of the ubiquitination and turnover of Mdm34 and Mdm12

Rsp5 modifies its substrates by adding a single ubiquitin moiety or short K63-linked polyubiquitin chains.[39] We therefore
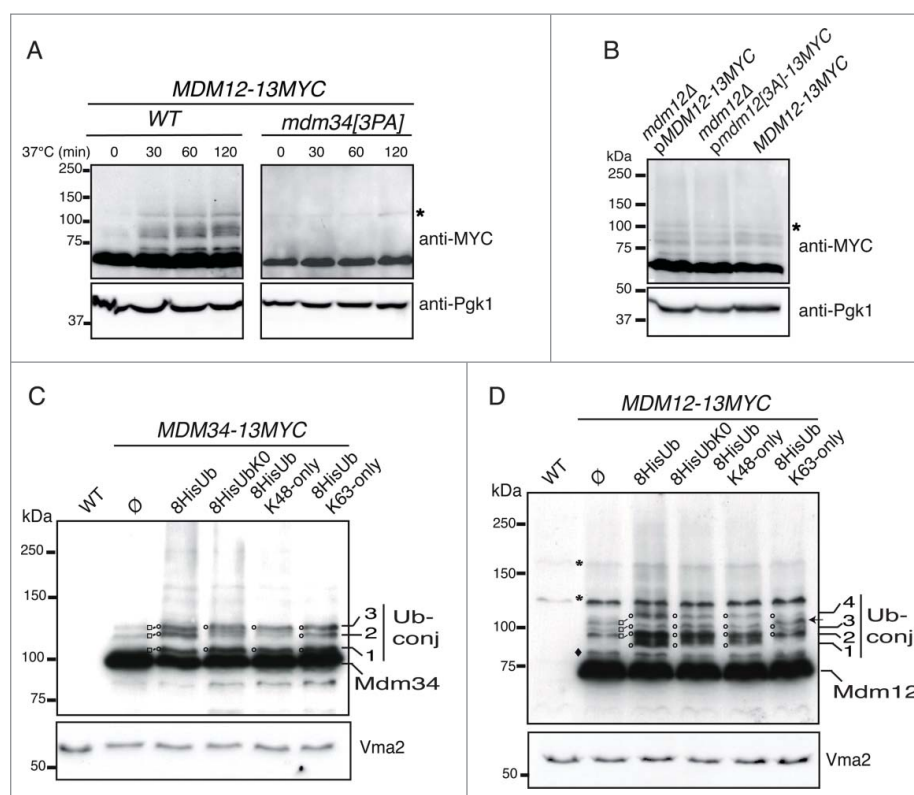
Figure 4. Analysis of the ubiquitination pattern of Mdm34, Mdm12 and PY mutants. (A) *MDM12-13MYC MDM34-FLAG* and *MDM12-13MYC/mdm34[3PA]-FLAG* cells were grown to early exponential growth phase in YPD at 24°C. They were then shifted to 37°C and total protein extracts were prepared at the times indicated. The ubiquitination pattern of Mdm12-13MYC was analyzed by western immunoblotting with antibodies against MYC and Pgk1. Pgk1 was used as a loading control. *, nonspecific band. (B) *mdm12Δ pMDM12-13MYC, mdm12Δ pmdm12[3PA]-13MYC* and the *MDM12-13MYC* strains were grown to late exponential growth phase to induce the ubiquitination of Mdm12. Total protein extracts were prepared and the ubiquitination pattern of Mdm12-13MYC was analyzed by western immunoblotting with antibodies against MYC and Pgk1 as a loading control. *, nonspecific band. (C and D) A wild-type strain without tagged genes (*WT*), and the *MDM12-13MYC* and *MDM34-13MYC* strains transformed with plasmids expressing 8-His tagged wild-type ubiquitin (8His-Ub), Ub-K0 (8His-UbK0), Ub-K48only (8HisUb-K48only), Ub-K63only (8HisUb-K63only) or with an empty plasmid (Ø) were grown to early exponential growth phase at 24°C in YNB with glucose as the carbon source. Cells were shifted to 37°C to induce protein ubiquitination and copper (CuSO4, 100 μM) was added to the cell cultures for 1 h to induce ubiquitin synthesis from the *CUP1* promoter. Total protein extracts were prepared and analyzed by western immunoblotting and autoradiography with antibodies directed against MYC (anti-MYC), ubiquitin (anti-Ub), or vacuolar membrane ATPase (anti-Vma2) as a loading control. Various slowly migrating bands are indicated by numbers. □, Mdm34-13MYC and Mdm12-13MYC ubiquitinated species; O, Mdm34-13MYC and Mdm12-13MYC 8His-ubiquitinated species; *, nonspecific bands; ◆, uncharacterized slowly migrating Mdm12-13MYC moiety;←, New band; Ub-conj, ubiquitin conjugated to Mdm34-13MYC and Mdm12-13MYC.

analyzed the conjugation of ubiquitin to Mdm34-MYC or Mdm12-MYC and used ubiquitin variants in which either 6 (K48-only or K63-only) or 7 (K0) of the lysine codons of ubiquitin had been mutated to arginine codons. We used an anti-ubiquitin antibody to confirm that ubiquitin was indeed overproduced (Fig. S4).

If a substrate is modified by the addition of K63-linked ubiquitin chains, then its polyubiquitination would be affected by the overproduction of UbK0 or UbK48-only, but not by the overproduction of UbK63-only. The K0 "lysine-less" ubiquitin can be conjugated to acceptor lysine residues in target substrates, but it blocks the elongation of polyubiquitin chains. In this context, a substrate subjected to monoubiquitination should show the same ubiquitination pattern regardless of the overproduction of wild type Ub, UbK0, UbK48-only or UbK63-only.

As previously shown (Fig. 1), 3 slowly migrating bands (Fig. 4C, Ub-conj) for Mdm34-13MYC were detected in the strain without ubiquitin overproduction (ø). These 3 bands corresponded to ubiquitin moieties, because their level increased and a shift in molecular weight was observed when the ubiquitin was tagged with histidine (Fig. 1 and 4C). The first and third

bands (Fig. 4C, bands 1 and 3) corresponded to monoubiquitinated Mdm34-13MYC, because they were also detected when the overproduced ubiquitin was K0 "lysine-less," K48-only or K63-only. The second band (Fig. 4C, band 2) was present when the overproduced ubiquitin was K63-only but its level decreased with UbK0 or UbK48-only, indicating that this band corresponded to a short K63-linked chain, probably di-ubiquitin. Thus, Mdm34 is mostly monoubiquitinated and has only short chains (probably di-ubiquitin) linked via lysine K63.

Mdm12-13MYC also presented 3 slowly migrating bands that corresponded to ubiquitin conjugates, as a shift in molecular weight was observed when overproduced ubiquitin was tagged with histidine (Fig. 4D, lane ø and His-Ub). Another band was present, just below the first ubiquitinated species (Fig. 4D, ◆), but this band did not correspond to ubiquitin because its level did not change upon ubiquitin overexpression and no shift in molecular weight was observed when ubiquitin was tagged with histidine. This band probably corresponds to a post-translational modification other than ubiquitination. The overproduction of wild-type, K0 or K48-only ubiquitin did not change the migration profiles of bands 2, 3 and 4 (Fig. 4D).

These bands therefore correspond to monoubiquitinated species. A new band (band 1) appeared when wild-type, K0 or K48-only ubiquitin was overproduced. However, when K63-only ubiquitin was overproduced, band 1 was not observed but another band appeared (Fig. 4D, arrow), indicating that Mdm12 was also modified by the addition of short K63-linked chains. Thus, Mdm34 and Mdm12 are probably monoubiquitinated on several acceptor lysine residues and also ubiquitinated with short K63-linked ubiquitin chains that are probably composed of 2 ubiquitin moieties. These findings are consistent with a role of Rsp5 in the ubiquitination of Mdm34 and Mdm12.

Unlike K48-linked polyubiquitination, and consistent with a nonproteasomal degradative role of Rsp5-mediated ubiquitination, these 2 types of ubiquitination do not efficiently target proteins for proteasomal degradation.[41] We analyzed the turnover of Mdm34, Mdm34[3PA] and Mdm12 in wild-type and *rsp5Δ* p*spt23ΔCT* strains (Fig. 5). Cells were grown to mid-exponential growth phase, transferred to 37°C to induce ubiquitination, and protein synthesis was inhibited by adding cycloheximide (CHX). The turnover of the different proteins was estimated by western blotting with immunodetection (Fig. 5). The decrease in the levels of Mdm34-MYC, Mdm34 [3PA]-MYC and Mdm12-MYC during the first part of the time course (0 to 1 h) was not significantly affected by the absence of Rsp5. After 2 to 4 h of CHX treatment, Mdm34[3PA]-MYC levels began to stabilize compared to wild type Mdm34-MYC. Furthermore, a weak stabilization of Mdm34-MYC and Mdm12-MYC was observed in the *rsp5Δ* p*spt23ΔCT* strain compared to the wild-type strain. Given these only late effects on stabilization, we conclude that, in the experimental conditions tested, the Rsp5-dependent ubiquitination of Mdm34 and Mdm12 was not involved in regulating the rapid turnover of these ERMES components.
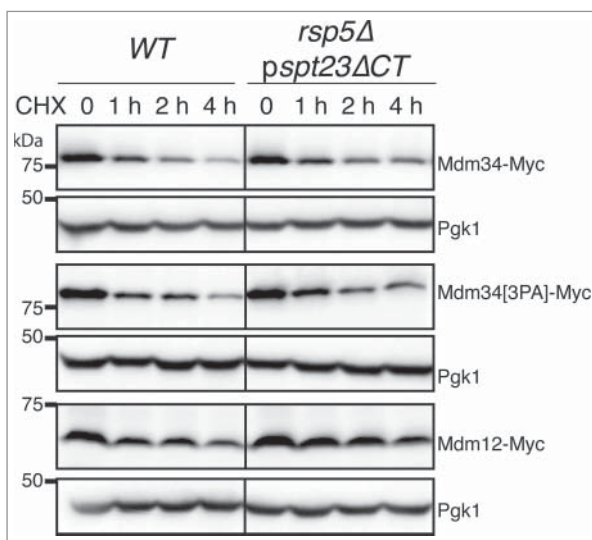
Figure 5. Analysis of the stability of the Mdm34, Mdm12 and mutant Mdm34[3PA] proteins. *WT* and *rsp5Δ* p*spt23ΔCT* strains bearing chromosomal genes encoding 9MYC-tagged *MDM34, mdm34[3PA]*, or *MDM12* were grown to mid-exponential growth phase in YPD at 24°C. The cells were then shifted to 37°C, and protein synthesis was blocked by adding cycloheximide (CHX, 200 µg/mL). Protein extracts were prepared at the times indicated and analyzed by western immunoblotting with an anti-MYC antibody. Pgk1 was used as a loading control.

The abolition of Mdm34 ubiquitination does not affect mitochondrial morphology or fission

The PY motif of Mdm34 is required for the Rsp5-dependent ubiquitination of both Mdm34 and Mdm12. An analysis of ERMES functions in cells in which this motif is mutated should provide insight into the role of Mdm12 and Mdm34 ubiquitination.

An absence of ERMES components greatly disturbs the organization of the mitochondria.[42-45] We therefore monitored the morphology of the mitochondria and ER, and the distribution of mtDNA, in wild-type and *mdm34[3PA]* strains. No differences were detected between wild-type and mutant cells (Fig. 6A). In particular, the mitochondria were closely associated with the ER and, consistent with normal growth of the *mdm34[3PA]* strain on glycerol media (Fig. S1A), the distribution of mtDNA, as assessed by DAPI staining, was unaffected in this mutant (Fig. 6A).

ERMES components have also been shown to serve as markers of mitochondrial division, consistent with a role in mitochondrial fission.[10] Furthermore, Mdm34 and Mdm12 are ubiquitinated under fission-inducing conditions. We therefore investigated whether the ubiquitination of these proteins was important for fission. We tested this hypothesis by investigating the fragmentation of mitochondrial networks in wild-type and *mdm34[3PA]* strains treated with α factor or H_2O_2 (Fig. 6B). In both sets of conditions, the degree of mitochondrial fragmentation was similar in the mutant and wild-type strains and the fragmented mitochondria were closely apposed to the ER in both strains (Fig. 6B).

We also compared the distributions of the Mdm34 and Mdm34[3PA] proteins tagged with GFP. Both strains grew normally on glucose- or glycerol-containing media, indicating that the GFP tag had no effect on Mdm34 function (Fig. S5). Mdm34-GFP and Mdm34[3PA]-GFP displayed punctate staining colocalized with mito-RFP–labeled mitochondria (Fig. 6C). The overall number of GFP foci was similar in the 2 strains, but the fluorescence intensity of these foci seemed to be slightly higher in the PY mutant.

The PY motif of Mdm34 is not required for ERMES assembly

Our results indicate that mutation of the PY motif of Mdm34, leading to lower levels of Mdm34 and Mdm12 ubiquitination, had no effect on mitochondrial or ER morphology, mtDNA distribution, mitochondrial fission or the distribution of Mdm34. However, this mutation resulted in a higher intensity of intracellular Mdm34-GFP foci. We therefore investigated the distribution of Mdm34 and its PY mutant, tagged with mCherry, relative to other ERMES components tagged with GFP (Fig. 7). Both Mmm1-GFP and Mdm12-GFP colocalized with Mdm34-mCherry, whether the PY motif was intact or mutated (Fig. 7). Moreover, mutation of the Mdm34 PY motif resulted in higher intensity of the signal for Mdm34[3PA]-mCherry and of the Mmm1 and Mdm12-GFP foci (Fig. 7). These results suggest that lower levels of Mdm34 and Mdm12 ubiquitination do not alter assembly of the ERMES complex, but may somehow affect the stabilization or dissociation of this complex.
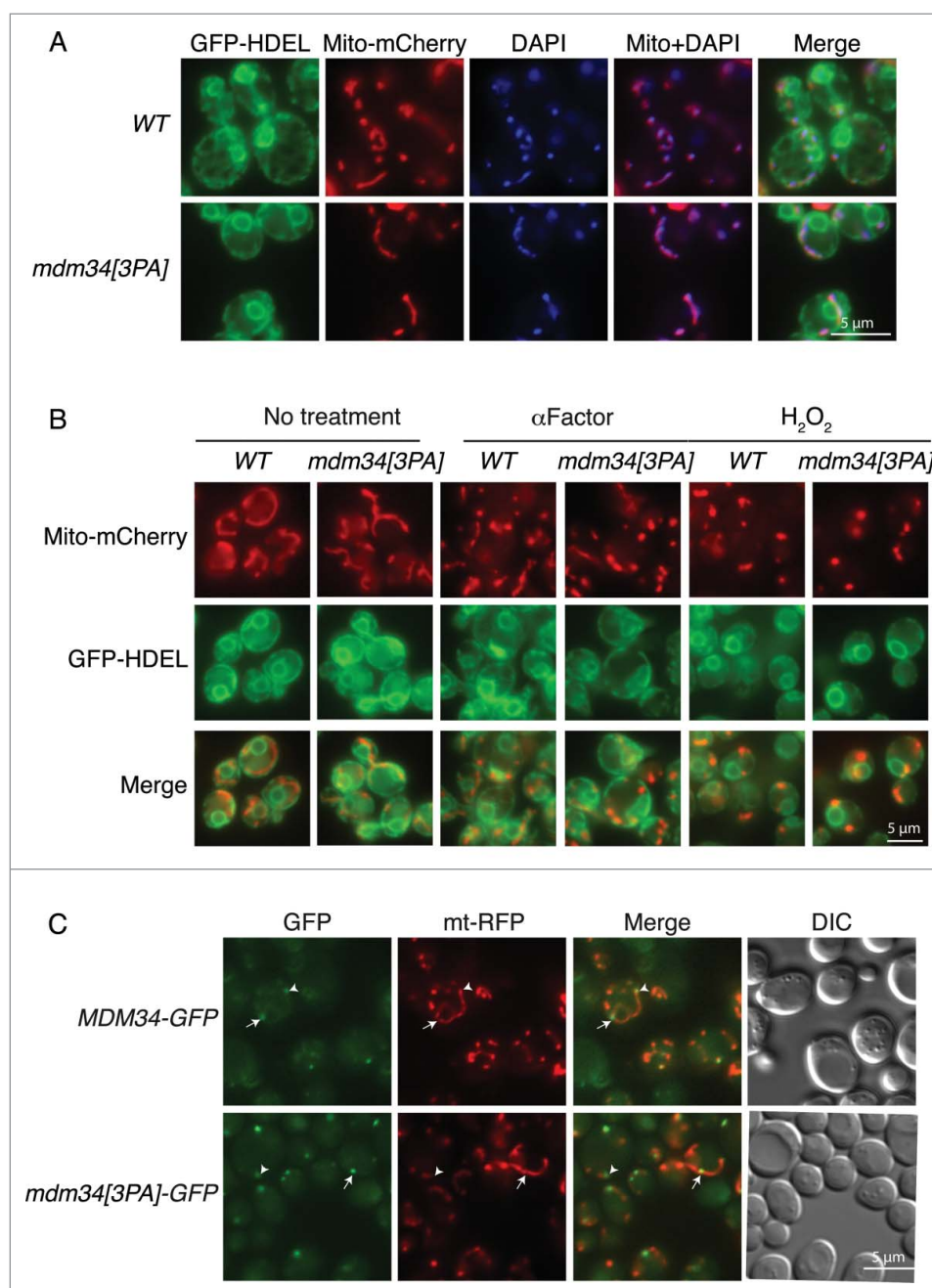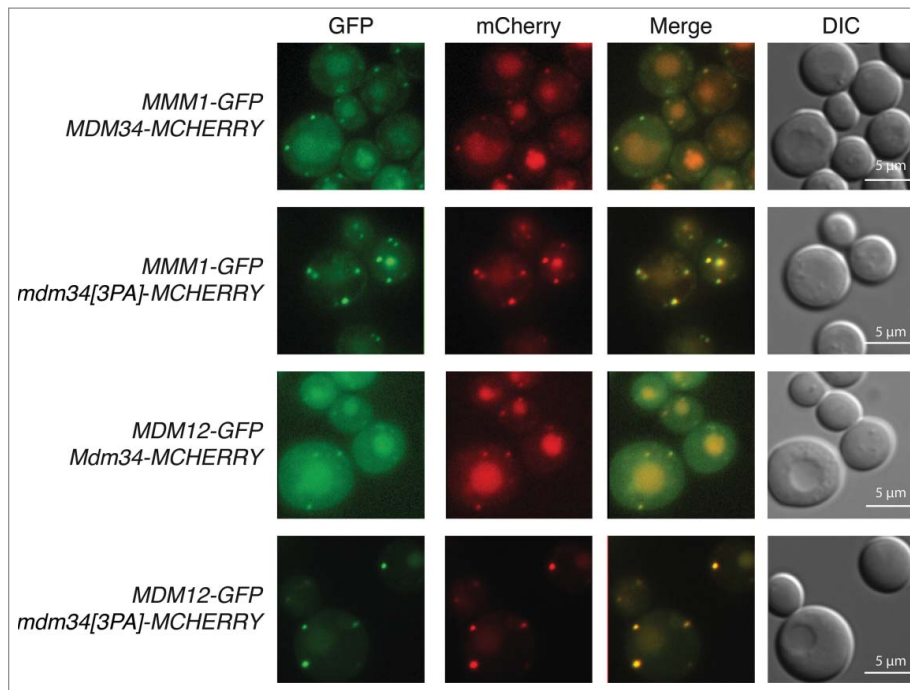
Figure 6. Mutation of the PY motif of Mdm34 does not affect ER or mitochondrial morphology, mitochondrial fission or Mdm34 localization. (A) *WT* or *mdm34[3PA]* strains bearing GFP-HDEL (ER marker) and Mito-mCherry expressed from vectors integrated into the chromosome were grown to early exponential growth phase in YPD at 30°C. Mitochondrial DNA was stained by adding 1 μg/mL DAPI to the growth medium and incubating for a further 2 to 3 h. Cells were washed twice and processed for fluorescence microscopy. (B) The same cells as in (A) were either left untreated (No treatment) or incubated with 50 μg/mL α factor for 3 h or with 2 mM H_2O_2 for 2 h. The cells were then washed twice and processed for fluorescence microscopy. (C) *MDM34-GFP* and *mdm34[3PA]-GFP* strains transformed with pYX142-mt-RFP were grown in YPD at 30°C before microscopy. Arrows indicate GFP at mitochondrial fission sites and arrowheads indicate GFP at mitochondrial tips. Cell shape was assessed with DIC.

We therefore investigated the behavior of Mdm34-GFP and its PY mutant in conditions stimulating the Rsp5-dependent ubiquitination of Mdm34 and Mdm12. H_2O_2 treatment, late exponential growth phase and heat shock resulted in weaker punctate staining for Mdm34-GFP, with an increase of GFP fluorescence in the vacuole (Fig. 8A and Fig. S6). By contrast, the PY mutation abolished this targeting of Mdm34-GFP to the vacuole. We used the vacuolar protease mutant *pep4Δ* to check that the green signal observed in the vacuole was due to the relative resistance of GFP to vacuolar

proteases (Fig. 8 and Fig. S6). In this mutant, defective for various vacuolar enzymes, the processing of GFP-tagged proteins is delayed and consequently the green signal in the vacuole is more intense. Consistent with this, *PEP4* deletion resulted in higher levels of GFP fluorescence in the vacuole, confirming the vacuolar accumulation of Mdm34-GFP in conditions inducing the ubiquitination of Mdm34 and Mdm12 (Fig. 8 and Fig. S6). Furthermore, we observed internal fluorescent structures in the vacuole of the *MDM34-GFP pep4Δ* strain (Fig. 8 and Fig. S6, structures indicated with

Figure 7. Mutation of the PY motif of Mdm34 does not affect the localization of Mdm12 and Mmm1. *MDM34-MCHERRY* and *MDM34[3PA]-MCHERRY* strains bearing chromosomal genes encoding *MDM12-GFP and MMM1-GFP* were grown to the exponential growth phase in glycerol-containing medium (YPG). Cells were washed twice and processed for fluorescence microscopy. Cell shape was assessed with DIC.

stars). Although less intense, GFP staining was also observed in the vacuole of the *mdm34[3PA]-GFP pep4Δ* strain, demonstrating that a small fraction of the protein, not visualized in a *PEP4* strain, was also targeted to the vacuole.

The PY motif of Mdm34 is required for efficient mitophagy

Our results suggest that the Rsp5-dependent ubiquitination of Mdm34 may target this protein to the vacuolar compartment for degradation. The ERMES complex has been implicated in the degradation of mitochondria by autophagy, and some components of the autophagic machinery are also degraded by autophagy. We therefore investigated whether the targeting of Mdm34 to the vacuole observed in conditions inducing ubiquitination also occurred in conditions triggering mitophagy. Growth on respiratory medium followed by nitrogen starvation induced the same PY-dependent accumulation of Mdm34-GFP in vacuoles as observed during the late exponential growth phase, and in conditions of redox stress and heat shock in both the presence and absence of *PEP4* (Fig. 8B). The vacuolar Mdm34-GFP signal detected after 4 h of nitrogen starvation was accompanied by a decrease in punctate staining in the cytosol, but both the vacuolar staining and the punctate signals in cytosol increased in intensity after 24 h (Fig. 8B). This suggests that, as reported for other factors involved in autophagy, the expression of Mdm34 may be upregulated to compensate for the targeting of this protein to the vacuole following the prolonged induction of mitophagy.[46] Moreover, the concentrated and highly fluorescent vacuolar structures seen upon *PEP4* inactivation accumulated after 24 h of nitrogen

starvation but were much less abundant when the Mdm34 PY motif was mutated. The morphology of these vacuolar structures is very similar to that of autophagosomes, the degradation of which is prevented by the inactivation of vacuolar peptidases. This further suggests that the Mdm34 PY motif and, thus, the Rsp5-dependent ubiquitination of Mdm34 and Mdm12, may affect the involvement of the ERMES complex in mitophagy.

We therefore investigated whether mitophagy was affected in the *mdm34[3PA]* mutant. In yeast cells, mitophagy can be induced by growth on a nonfermentable carbon source to enhance mitochondrial mass, and treatment with rapamycin, which mimics nitrogen starvation by inactivating the Tor kinase pathway, or by long periods of incubation in stationary phase (2 to 3 d).[47-49] Rapamycin inactivates the Tor pathway and induces many cellular responses, including autophagy. We assessed the growth of 2 different (GFP or MYC-tagged) PY mutants of *MDM34* on glycerol-containing medium supplemented with 5 or 10 nM rapamycin (Fig. 9A). The 2 PY mutants were clearly sensitive to rapamycin treatment.

We then used growth on glycerol-containing medium followed by rapamycin treatment to analyze mitophagy with the pH-sensitive biosensor mtRosella, which can be used for the direct detection of mitophagy.[50] MtRosella has a mitochondrial targeting signal at its N terminus, followed by the red fluorescent protein (DsRed) sequence, fused in tandem with a pH-sensitive GFP (pHLuorin). MtRosella labels mitochondria with overlapping green and red fluorescence (Fig. 9B).[50] Upon the induction of mitophagy by rapamycin, mitochondria are targeted to the vacuole, where the green GFP signal of mtRosella is lost due to the low pH of the vacuole, such that only the red signal remains (Fig. 9B, white arrows).[50] After one d of
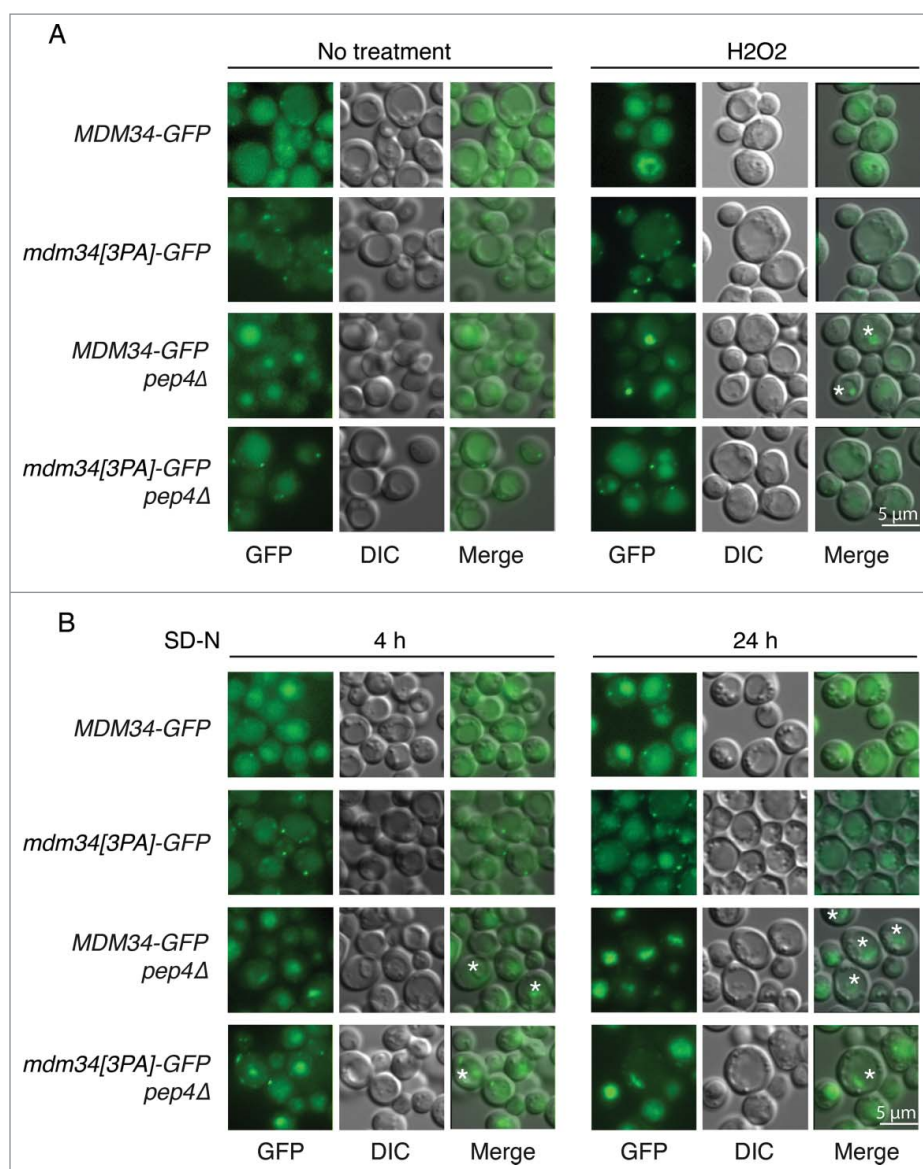
Figure 8. Analysis of Mdm34-GFP localization in conditions inducing ubiquitination and mitophagy. (A) *MDM34-GFP, mdm34[3PA]-GFP, MDM34-GFP pep4Δ* and *mdm34 [3PA]-GFP pep4Δ* strains were grown to exponential growth phase in complete synthetic medium. The cells were divided into 2 sets. The first set was treated with 2 mM H_2O_2 for 2 h (A) and the second set was washed 3 times with water and the cells were resuspended in SD-N medium and cultured for 4 or 24 h (B). GFP fluorescence was analyzed with a GFP filter set and cell morphology was investigated with DIC. Fluorescent structures inside the vacuole are indicated by a star symbol (*).

rapamycin treatment, some red signal was visible in the vacuoles of wild-type (*WT*) cells (∼50% of vacuoles with a red signal). The percentage of cells with red vacuoles was lower in the *mdm34[3PA]* mutant than in the wild type (∼30% of vacuoles with a red signal). The PY motif of Mdm34 and, consequently, the Rsp5-dependent ubiquitination of Mdm34 and Mdm12, are therefore required for efficient mitophagy. However, prolonged culture of the yeast cells induced vacuolar auto-fluorescence, hampering the detection of red vacuoles. Thus, the extent of mitophagy inhibition in the *mdm34[3PA]* mutant may have been underestimated.

Once in the vacuole, mtRosella is cleaved, giving rise to a free GFP moiety resistant to degradation. A more quantitative approach to the analysis of mitophagy involves the use of western immunoblotting to detect the generation of free GFP.[14] We thus monitored the processing of mtRosella in *WT* and *mdm34 [3PA]* cells. After 24 h of rapamycin treatment, mtRosella levels decreased in the *WT* strain and this decrease was accompanied by an increase in free GFP levels (Fig. 9C left). The level of mitophagy, assessed by calculating the ratio of % free GFP: (free GFP + mtRosella), in the *mdm34[3PA]* mutant was much lower than that in *WT* cells (Fig. 9C). As rapamycin blocks the initiation of translation, we were able to analyze the half-life of Mdm34-MYC in these conditions (Fig. 9C, left and upper panel). In this context, wild-type Mdm34-MYC levels decreased more rapidly than those of the PY mutant, consistent with our observation that Mdm34 was targeted to the vacuole, probably together with the mitochondria, during mitophagy. Mitophagy is also induced after long periods of incubation (2 to 3 d) in a postexponential growth phase.[48,49] In such conditions of starvation, the free GFP: (Free GFP + mtRosella) ratio in the *mdm34[3PA]* mutant was also lower than that in the WT, confirming the necessity of the PY motif of Mdm34 for efficient mitophagy (Fig. 9C, right panel).
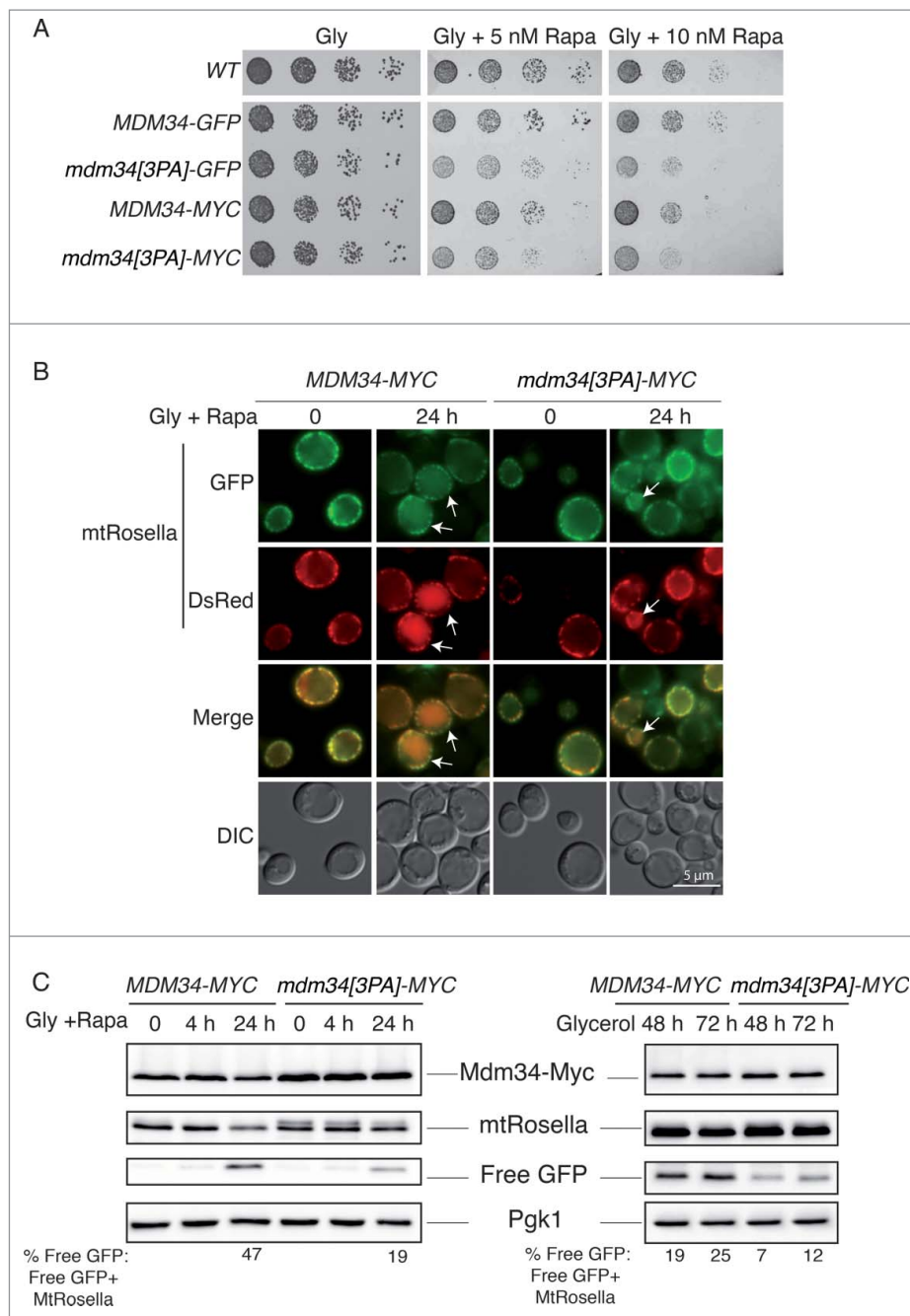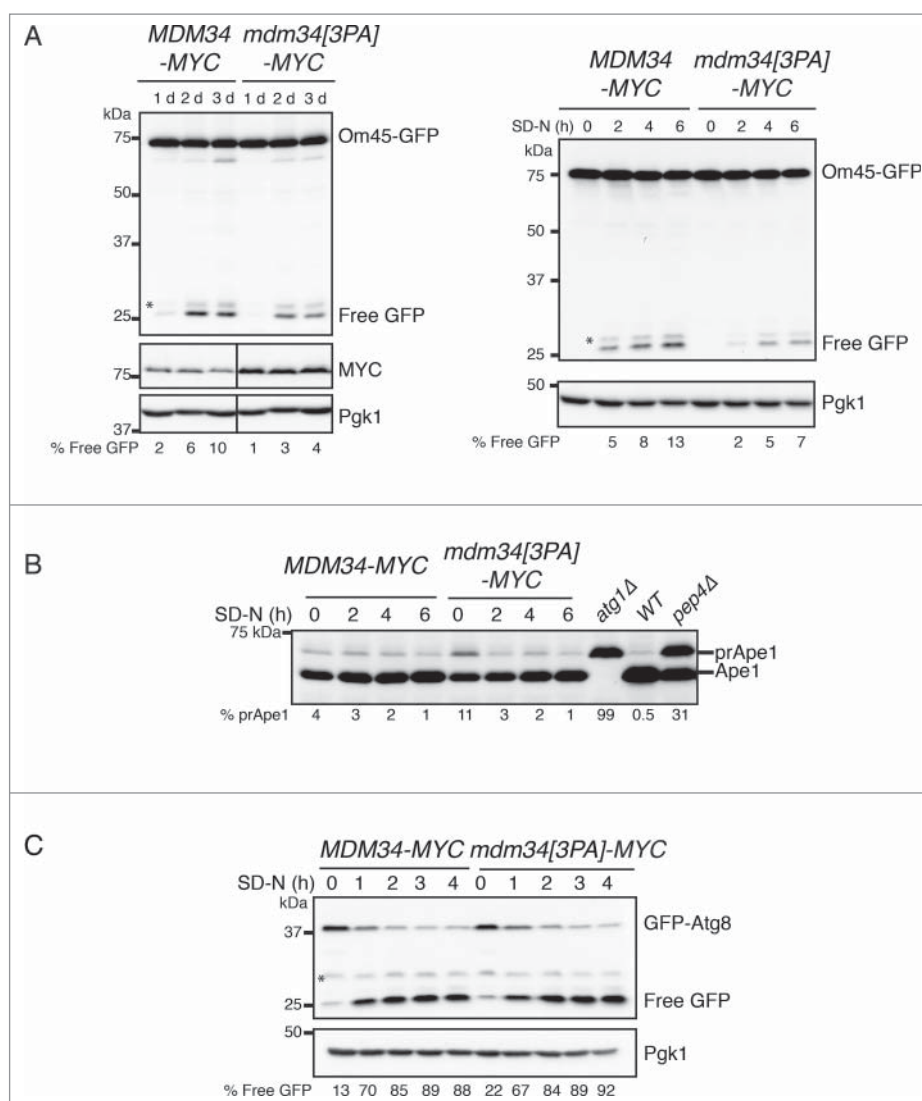
Figure 9. Mutation of the PY motif of *MDM34* affects mitophagy. (A) The WT, *MDM34-GFP*, *mdm34[3PA]-GFP*, *MDM34-MYC* and *mdm34[3PA]-MYC* strains were grown to mid-exponential growth phase in YPD, washed twice in water and subjected to serial 5-fold dilution. Cells were then spotted onto solid complete medium containing glycerol as a carbon source (Gly) and supplemented with the indicated concentrations of rapamycin (Rapa). The plates were then incubated at 30°C. (B and C) The *MDM34-MYC* and *mdm34[3PA]-MYC* strains transformed with a plasmid encoding mitochondrion-targeted Rosella (mtRosella) were grown to very early exponential growth phase in YNB with glycerol as the carbon source and supplemented with the appropriate amino acids. After 24 h in glycerol-containing medium, the cultures were split in 2: one-half of the culture was treated with 200 nM rapamycin (Rapa) to induce mitophagy and the second-half of the culture was allowed to grow for 48 to 72 h. The cells of the first half of the culture were observed by fluorescence microscopy at time 0 (just before the addition of rapamycin) and after 24 h in the presence of rapamycin (A). Arrows indicate cells with mtRosella in the vacuole. (C) Total protein extracts were obtained from these cells after 0, 4 and 24 h of rapamycin treatment (C, left panel) and from the cells of the second culture after 48 and 72 h of culture in glycerol-containing medium (C, right panel). Protein extracts were analyzed by western immunoblotting with antibodies against MYC, GFP (to detect full-length mtRosella and free GFP) and Pgk1, as a loading control. The ratio of free GFP to mtRosella was determined by densitometry with Image Lab 3.0.1 software (Bio-Rad). Fluorescence images and protein gel blots shown were representative images from 3 independent experiments.

Crosstalk between ERMES, ubiquitination and mitophagy

The monitoring of mtRosella indicated that mutation of the PY motif of *MDM34* reduced mitochondrial targeting to the vacuole by a factor of 2. However, some technical limitations were observed for the western blot analysis of mtRosella (Fig. S7). A large number of degradative bands were observed when the cells were grown in the presence of rapamycin and during stationary phase (Fig. S7, bands are numbered). Nonetheless, the percentage of free GFP was consistently higher in the wild-type strain than in the *mdm34[3PA]* mutant. We thus analyzed mitophagy following the processing of GFP-tagged mitochondrion-resident

Figure 10. Mutation of the PY motif of *MDM34* affects mitophagy but not nonselective bulk autophagy. (A and B). The *MDM34-MYC OM45-GFP* and *mdm34[3PA]-MYC OM45-GFP* strains were grown to early exponential growth phase in YNB with glycerol as the carbon source and supplemented with the appropriate amino acids. After one d in glycerol-containing medium, the cultures were split in 2: one half of the culture was left untreated for 3 d (A left part) and the other was washed 3 times with water and resuspended in SD-N medium and incubated for 2, 4 and 6 h (A, right panel and B). Protein extracts from *atg1Δ*, *pep4Δ* and a wild-type (WT) strain cultured to exponential growth phase in YPG were also prepared (B). Total protein extracts were prepared and analyzed by western immunoblotting with antibodies against GFP (to detect full-length OM45-GFP and free GFP), MYC, Ape1 and Pgk1, as a loading control. *MDM34-MYC* and *mdm34[3PA]-MYC* strains, transformed with p*GFP-ATG8*, were grown as in (B) and protein extracts were analyzed by western immunoblotting with anti-GFP and anti-Pgk1 antibodies. The percentage of Free GFP corresponds to the ratio free GFP: (free GFP + Om45-GFP) (A) or free GFP: (free GFP + GFP-Atg8) (C). The percentage of prApe1 corresponds to the ratio prApe1: prApe1+Ape1. *, nonspecific band.

proteins upon the induction of autophagy, to confirm the results obtained with mtRosella. As expected, processing levels for the endogenous outer membrane protein Om45-GFP were lower in the *mdm34[3PA]* mutant after the induction of mitophagy, both in stationary phase and upon nitrogen starvation (Fig. 10A).

The same defect was observed with the endogenous matrix-resident chaperone Hsp78-GFP, a protein that displays partial colocalization with Mdm34[51] (Fig. S8). These results confirm that mutation of the PY motif of Mdm34 decreases mitochondrial degradation by autophagy and suggest that the Rsp5-dependent ubiquitination of Mdm34 and Mdm12 is required for efficient mitophagy.

In this context, Rsp5 inactivation would be expected to mimic the effect of the *mdm34[3PA]* mutation on the processing of Om45-GFP upon nitrogen starvation. However, the *rsp5Δ* p*spt23ΔCT* strain is unable to grow on nonfermentable

media, such as glycerol and lactate, and such culture is required to increase mitochondrial mass and to induce mitophagy (Fig. S9A). The cells grew poorly in galactose-containing medium but normally in medium supplemented with raffinose, a poorly fermentable carbon source on which respiration is derepressed (Fig. S9A). Mitochondrial porin (Por1) levels were higher in raffinose-containing medium than in glucose-containing media, suggesting an increase in mitochondrial mass (Fig. S9B). We therefore analyzed mitophagy in the *rsp5Δ* p*spt23ΔCT* mutant grown in raffinose-containing medium at 25°C. Unlike nitrogen starvation after culture in nonfermentable conditions, the nitrogen starvation occurring after growth in raffinose-containing medium led to a progressive increase in the amount of Om45-GFP (Fig. S9C). Moreover, the presence of free GFP, and, therefore, the induction of mitophagy, was not detected until 24 h of starvation (*vs.* 2 h for cells initially
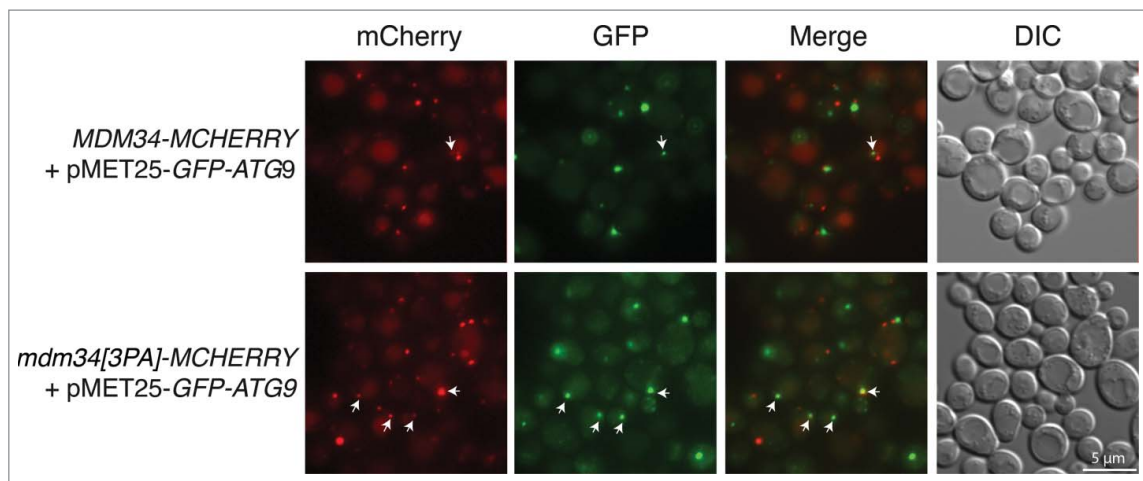
Figure 11. Analysis of *GFP-ATG9* localization in the *WT* and mutant *MDM34[3PA]* strains. *MDM34-MCHERRY* and *MDM34[3PA]-MCHERRY* strains transformed with p*MET25-GFP-ATG9* were cultured in minimal medium containing glycerol and then transferred to SD-N medium for 1 h for the induction of starvation. Cells were then imaged for the assessment of mCherry (Red) and GFP (Green) fluorescence, and cell shape was visualized with DIC. The arrows indicate the colocalization of red and green signals.

cultured on glycerol at 30°C), when Om45-GFP levels were higher (Fig. S9C). In these conditions, Om45-GFP processing rates were, nevertheless, significantly lower in the *rsp5Δ* p*spt23ΔCT* mutant than in the wild-type strain, 24 h and 48 h after the induction of starvation (Fig. S9C). Thus, like the *mdm34[3PA]* mutation, the absence of *RSP5* results in delayed mitophagy.

Specificity of ERMES ubiquitination in mitophagy

Our results indicate that the Rsp5-mediated ubiquitination of Mdm34 and Mdm12 is required for efficient mitophagy. We therefore investigated whether the inactivation of Rsp5 or mutation of the PY motif of Mdm34 affected other selective or bulk autophagy-dependent processes. The cytoplasm-to-vacuole targeting (Cvt) pathway is considered to be a selective type of autophagy mediating the delivery of the precursors of the vacuolar hydrolases aminopeptidase I (prApe1) and α-mannosidase (prAms1) from the cytosol to the vacuole (for a review see).[52] In the vacuole, prApe1 is activated by processing to generate a mature form of the protein (Ape1). This selective trafficking pathway, which requires several components involved in autophagy, occurs under nutrient-rich conditions, but the transport and vacuolar processing of Ape1 are further stimulated by starvation and the induction of autophagy. Growth in raffinose followed by nitrogen starvation stimulated the processing of prApe1, and this processing was moderately affected by the absence of *RSP5* (Fig. S9C), but not by mutation of the PY motif of *MDM34* (Fig. 10B). However, at time 0, before the initiation of starvation, there was more prApe1 in the *rsp5Δ* p*spt23ΔCT* and *mdm34[3PA]* mutants than in the wild-type strain. We conclude that the Rsp5-dependent ubiquitination of Mdm34 may control prApe1 processing in constitutive conditions, but that it is not involved in regulating the Cvt pathway following the induction of autophagy. Finally, neither *rsp5*[53] nor *mdm34[3PA]* mutations affected the processing of GFP-Atg8, a marker for bulk autophagy and a component of autophagosomes, under nitrogen starvation conditions (Fig. 10C). Thus, the ubiquitination of Mdm34 and Mdm12 was not involved in the core activity of autophagy, instead playing a

more specific role in mitophagy and, to a lesser extent, in the Cvt pathway.

Crosstalk between ERMES ubiquitination and factors involved in autophagy

Overall, our results demonstrate that the Rsp5-dependent ubiquitination of Mdm34 and Mdm12 is required for efficient mitophagy. We thus investigated whether mutation of the PY motif affected the cellular distribution of Mdm34 relative to components of the autophagy machinery shown to be essential for mitophagy (Fig. 11 and Fig. S10). For this purpose, the cellular distributions of the Mdm34 and Mdm34[3PA] proteins fused to mCherry were analyzed upon mitophagy induction, in cell co-expressing the mitophagy receptor GFP-Atg32, and the ubiquitin-like GFP-Atg8 present on autophagosomal membranes or GFP-Atg9, the only integral membrane protein of the Atg family of proteins. As expected from its predicted role in the delivery of lipids to the autophagosome,[14] Mdm34-mCherry colocalized with GFP-Atg32, GFP-Atg8 and GFP-Atg9 (Fig. 11 and Fig. S10). Mutation of the PY motif of Mdm34 did not affect the colocalization of Mdm34 with Atg32 or Atg8. However, the mutant Mdm34[3PA]-mCherry protein was more frequently colocalized with GFP-Atg9 than the wild-type Mdm34-mCherry (Fig. 11, colocalization indicated with arrows). Atg9 is a transmembrane protein considered to act as a potential membrane carrier, transporting membranes from other organelles to the phagophore to facilitate nucleation and/or expansion of the autophagosome.[54] The colocalization of GFP-Atg9 and Mdm34[3PA]-mCherry puncta thus suggests that inhibition of the ubiquitination of Mdm34 and Mdm12 may lead to Atg9 being sequestered or stabilized at contact sites between the mitochondria and the endoplasmic reticulum.

Discussion

We show here that Mdm34 and Mdm12, 2 components of the ERMES complex, are ubiquitinated by the E3 ligase Rsp5. This ubiquitination was induced, in media containing glucose or

glycerol, in conditions triggering mitochondrial fission. However, a mutation of *MDM34* interfering with the ubiquitination of both Mdm34 and Mdm12 did not inhibit mitochondrial fragmentation. We further demonstrated that Rsp5-dependent ubiquitination was not involved in promoting the turnover of Mdm34 and Mdm12. Instead, it was involved in the degradation of mitochondria by autophagy. These findings reveal a new role for Rsp5 in mitophagy.

A previous study has identified Mdm34 as a potential substrate of the ubiquitin ligase Mdm30.[20] However, Ota et al. show that deletion of *MDM30* only partly decreases Mdm34 ubiquitination, indicating the probable involvement of another ubiquitin ligase. We found that *MDM30* deletion did not decrease or abolish the ubiquitination of Mdm34. This discrepancy with the findings of Ota *et al.* probably results from differences in the technical approaches used.[20] The strains used in the 2 studies were of different backgrounds, and we used 9 and 13-MYC rather than the T7 epitope for the C-terminal tagging of Mdm34. With this T7 epitope, Ota et al. are unable to detect Mdm34 in whole-cell extract and are forced to use mitochondria-enriched fractions. With the MYC epitope, we were able to visualize Mdm34 in whole-cell extracts and the ubiquitination of this protein may have been better preserved in cells lacking *MDM30*.

Previous studies have identified Mdm34 as a potential binding partner of Rsp5, but the ubiquitination of Mdm34 is not documented.[35,36] Here, we demonstrate that Rsp5 promotes the ubiquitination of both Mdm34 and Mdm12. However, Rsp5 did not seem to target the other ERMES components, Mmm1, Mdm10 and Gem1. The PY motif of Mdm34 was found to be essential for the ubiquitination of both Mdm34 and Mdm12, as its mutation, and not the mutation of the potential PY motif of *MDM12*, abolished the ubiquitination of both proteins. This suggests that Mdm34 may be a direct target of Rsp5 involved in the recruitment of the ligase to the contact sites between the ER and the mitochondria.

We showed that, in the experimental conditions tested, the ubiquitination of Mdm34 and Mdm12 did not regulate the rapid turnover of these proteins. While our paper was under revision, another group published results confirming our observations concerning the ubiquitination of Mdm34 by Rsp5 and the role of the PY motif in this post-translational modification.[55] However, in their experimental conditions, Wu et al. observe very high levels of Mdm34 polyubiquitination (polyubiquitinated chains >170 kDa), which are implicated in the rapid turnover of the protein.[55] Their results do not conflict with those presented here but they indicate that the length of ubiquitin chains may change the fate of Mdm34. We showed that Mdm34 and Mdm12 undergo multi-monoubiquitination and short-chain K63 polyubiquitination, modifications that do not promote efficient targeting to the proteasome.[41] The regulation of the ubiquitination status of Mdm34 therefore probably involves the editing of Rsp5-mediated ubiquitination by ubiquitin proteases (DUBs), which restrict the elongation of ubiquitin chains. Ubp2 is a DUB that physically interacts with Rsp5, counteracting its activity by trimming the chains added by the ligase, to yield monoubiquitinated substrates.[56] Ubp3 is another ubiquitin protease that deubiquitinates Sec23, a protein

target of Rsp5.[57] Ubp3 has recently been identified as a positive regulator of autophagy and a negative regulator of mitophagy.[34] Atg19, a receptor for the Cvt pathway, is ubiquitinated and subject to deubiquitination by Ubp3.[58] The substrates of Ubp3 for mitophagy remain to be identified and the identification of a DUB enzyme acting on Mdm34 and Mdm12 would clearly help to clarify the role of Mdm34 and Mdm12 ubiquitination in mitophagy and proteasomal degradation.

Stress conditions inducing mitochondrial fission also stimulated the ubiquitination of Mdm34 and Mdm12 and induced the targeting of Mdm34 to the vacuole. Conversely, the inhibition of ERMES component ubiquitination observed in the *mdm34[3PA]* mutant affected the targeting of Mdm34 to the vacuole, thereby delaying the induction of mitophagy, but not mitochondrial fragmentation. However, it remains unclear how ubiquitination mediates mitophagy.

Rsp5 has recently been shown to ubiquitinate polyQ proteins, which are recognized by the ubiquitin-binding CUE-domain protein Cue5.[53] Cue5 was the first ubiquitin-Atg8 receptor to be identified in yeast and to be shown to function in the ubiquitin-dependent autophagy of aggregation-prone proteins. It is tempting to speculate that the recruitment of Rsp5 to contact sites between the ER and mitochondria promotes the ubiquitination of Mdm34 and Mdm12, thereby promoting the recruitment of Cue5 or another ubiquitin-binding protein and facilitating the recruitment of the autophagy machinery. A defect in the stability or turnover of the ERMES complex might therefore affect mitophagy, as observed in the *mdm34[3PA]* mutant. In this context, Mdm34 may act as a mitophagy receptor independent of Atg32, for the recruitment of Atg8 and Rsp5 may thus accomplish a function similar to PARK2/Parkin in mitophagy.

It has been suggested that ERMES components supply lipids to the growing autophagosomes during mitophagy.[14] Our results show that the ubiquitination of Mdm34 and Mdm12 is important not only for mitophagy, but may also regulate the Cvt pathway in nutrient-rich conditions. We have also shown that the core autophagy machinery is not affected (normal GFP-Atg8 processing and localization) and that the mitophagy receptor GFP-Atg32 is not mislocalized upon mutation of the PY motif of Mdm34. However, we observed a higher level of GFP-Atg9 colocalization with the Mdm34[3PA] mutant, consistent with a role for ERMES in autophagosome biogenesis. Atg9 is an integral membrane protein that cycles between the PAS (phagophore assembly site), mitochondria and other cytoplasmic pools.[54] Mutation of the PY motif of Mdm34 may affect the trafficking of Atg9, thereby affecting autophagosome biogenesis. Further experiments are required to determine how this could be achieved.

Materials and methods

Yeast strains and plasmid constructs

The yeast plasmids and strains used in this study are listed in Tables 1 and 2. Except for *mdm12Δ* and *atg1Δ* (BY4741 background), all yeast strains are derivatives of W303 or DF5.[59] DNA manipulations, including restriction

Table 1. Yeast strains.

N°	Yeast name or other name	Yeast genotype	Source/Ref
608	WT/DF5	Mat a; his3-Δ200; leu 2-3,112; lys2-801; trp1-1 (am); ura3-52	[37]
607	rsp5Δ pspt23ΔCT	Mat a; his3-Δ200; leu 2-3,112; lys2-801; trp1-1 (am); ura3-52; rsp5::HIS3; pSPT23[1-686]-URA3	[37]
396	WT/MHY501	Mat alpha, his3-Δ200; leu 2-3,112; lys2-801; trp1-1 (am); ura3-52	[70]
837	MDM34-MYC	Mat a; his3-Δ200; leu 2-3,112; lys2-801; trp1-1 (am); ura3-52; MDM34-9MYC::KANMX4	This study
846	MDM34-MYC rsp5Δ pspt23ΔCT	Mat a; his3-Δ200; leu 2-3,112; lys2-801; trp1-1 (am); ura3-52; MDM34-9MYC::KANMX4; rsp5::HIS3; pSPT23[1-686]-URA3	This study
855	MDM34[3PA]-MYC	Mat a; his3-Δ200; leu 2-3,112; lys2-801; trp1-1 (am); ura3-52; MDM34AAAY-9Myc::KANMX4	This study
853	MMM1-MYC	Mat a; his3-Δ200; leu 2-3,112; lys2-801; trp1-1 (am); ura3-52; can1-100; MMM1-9MYC::KANMX4	This study
866	MMM1-MYC rsp5Δ pspt23ΔCT	Mat a; his3-Δ200; leu 2-3,112; lys2-801; trp1-1 (am); ura3-52; can1-100; MMM1-9MYC::KANMX4; rsp5::HIS3; pSPT23[1-686]-URA3	This study
854	MDM12-MYC	Mat a; his3-Δ200; leu 2-3,112; lys2-801; trp1-1 (am); ura3-52; MDM12-9MYC::KANMX4	This study
856	GEM1-MYC	Mat a; his3-Δ200; leu 2-3,112; lys2-801; trp1-1 (am); ura3-52; GEM1-9MYC::KANMX	This study
858	MDM10-MYC	Mat a; his3-Δ200; leu 2-3,112; lys2-801; trp1-1 (am); ura3-52; MDM10-9MYC::KANMX4	This study
867	MDM12-MYC rsp5Δ pspt23ΔCT	Mat a; his3-Δ200; leu 2-3,112; lys2-801; trp1-1 (am); ura3-52; MDM12-9MYC::KANMX4; rsp5::HIS3; pSPT23[1-686]-URA3	This study
871	MDM10-MYC rsp5Δ pspt23ΔCT	Mat a; his3-Δ200; leu 2-3,112; lys2-801; trp1-1 (am); ura3-52; MDM10-9MYC::KANMX4; rsp5::HIS3; pSPT23[1-686]-URA3	This study
1005	MDM12-13MYC MDM34-FLAG	Mat a; his3-Δ200; leu 2-3,112; lys2-801; trp1-1 (am); ura3-52; MDM12-13MYC::HIS3MX6; MDM34-3FLAG::KANMX4	This study
1006	MDM12-13MYC MDM34[3PA]-FLAG	Mat a; his3-Δ200; leu 2-3,112; lys2-801; trp1-1 (am); ura3-52; MDM12-13MYC::HIS3MX6, MDM34AY-3FLAG::KANMX4	This study
1093	MDM34-13MYC	Mat a; his3-Δ200; leu 2-3,112; lys2-801; trp1-1 (am); ura3-52; MDM34-13MYC::HIS3MX6	This study
1094	MDM34[3PA]-13MYC	Mat a; his3-Δ200; leu 2-3,112; lys2-801; trp1-1 (am); ura3-52; MDM34AAAY-13MYC::HIS3MX6	This study
1004	MDM12-13MYC	Mat a; his3-Δ200; leu 2-3,112; lys2-801; trp1-1 (am); ura3-52; MDM12-13MYC::HIS3MX6	This study
997	WT GFP-HDEL MITO-MCHERRY	Mat a; his3-Δ200; leu 2-3,112::MITO-MCHERRY:LEU2; lys2-801; trp1-1::GFP-HDEL:TRP; ura3-52	This study
1009	MDM34[3PA] GFP-HDEL MITO-MCHERRY	Mat a; his3-Δ200; leu 2-3,112::MITO-MCHERRY:LEU2; lys2-801; trp1-1::GFP-HDEL:TRP; ura3- 52; MDM34AAAY::HIS3	This study
793	MDM34-GFP	Mat a; his3-Δ200; leu 2-3,2-112; lys2-801; trp1-1(am); ura 3-52; MDM34-GFP::KlTRP1	This study
889	MDM34[3PA]-GFP	Mat a; his3-Δ200; leu 2-3,112; lys2-801; trp1-1(am); ura3-52; MDM34AAAY-GFP::KANMX4	This study
1112	MDM34-GFP pep4Δ	Mat a; his3-Δ200; leu 2-3,112; lys2-801; trp1-1(am); ura3-52; MDM34-GFP::KlTRP1; pep4:: NATNT2	This study
1113	MDM34[3PA]-GFP pep4Δ	Mat a; his3-Δ200; leu 2-3,112; lys2-801; trp1-1(am); ura3-52; MDM34AAAY-GFP::KANMX4	This study
1080	MDM34-MCHERRY	Mat a; ura3-1; trp1-1; leu2-3,112; his3-11,15; can1-100; MDM34-MCHERRY::KANMX4	This study
1081	MDM34[3PA]-MCHERRY	Mat a; ura3-1 trp1-1 leu2-3,112 his3-11,15 can1-100; MDM34AAAY-MCHERRY::KANMX4	This study
1085	MDM34-MCHERRY MDM12-GFP	Mat a; ura3-1; trp1-1; leu2-3,112; his3-11,15; can1-100; MDM34-MCHERRY::KANMX4; MDM12-GFP::TRP	This study
1086	MDM34[3PA]-MCHERRY MDM12-GFP	Mat a; ura3-1; trp1-1; leu2-3,112; his3-11,15; can1-100; MDM34AAAY-MCHERRY::KANMX4; MDM12-GFP::TRP	This study
1087	MDM34-MCHERRY MMM1-GFP	Mat a; ura3-1; trp1-1; leu2-3,112; his3-11,15; can1-100; MDM34-MCHERRY::KANMX4; MMM1-GFP::TRP	This study
1088	MDM34[3PA]-MCHERRY MMM1-GFP	Mat a; ura3-1; trp1-1; leu2-3,112; his3-11,15; can1-100; MDM34AAAY-MCHERRY::KANMX4 ; MMM1-GFP ::TRP	This study
1096	MDM34-MCHERRY MET25-GFP-ATG32	Mat a; ura3-1; trp1-1; leu2-3,112; his3-11,15; can1-100; MDM34-MCHERRY::KANMX4; NATNT2::MET25-GFP-ATG32	This study
1097	MDM34[3PA]-MCHERRY MET25-GFP-ATG32	Mat a; ura3-1; trp1-1; leu2-3,112; his3-11,15; can1-100; MDM34-MCHERRY::KANMX4; NATNT2::MET25-GFP-ATG32	This study
892	MDM34-MYC mdm30Δ	Mat a; his3-; leu 2-3,112; lys2-801; trp1-1; ura3-52; MDM34-9MYC::KANMX4; mdm30::HIS5	This study
869	GEM1-MYC rsp5Δ pspt23ΔCT	Mat a; his3-Δ200; leu2-3, 2-112; lys2-801; trp1-1(am); ura3-52; rsp5::HIS3; GEM1-9MYC::KANMX4; pSPT23[1-686]-URA3	This study
1051	mdm12Δ	Mat a; his3Δ1; leu2Δ0; met15Δ0; ura3Δ0; mdm12::KANMX4	Euroscarf
1091	atg1Δ	Mat a; his3Δ1; leu2Δ0; met15Δ0; ura3Δ0; atg1::KANMX4	Euroscarf
1075	MDM34-MYC OM45-GFP	Mat a; his3-Δ200; leu 2-3,112; lys2-801; trp1-1(am); ura3-52; MDM34-9MYC::KANMX; OM45-GFP::TRP	This study
1076	MDM34[3PA]-MYC OM45-GFP	Mat a; his3-Δ200; leu 2-3,112; lys2-801; trp1-1(am); ura3-52; MDM34AAAY-9MYC::KANMX; OM45-GFP::TRP	This study
1137	MDM34-MYC HSP78-GFP	Mat a; his3-Δ200; leu 2-3,112; lys2-801; trp1-1(am); ura3-52; MDM34-9MYC::KANMX; HSP78-GFP::TRP	This study
1138	MDM34[3PA]-MYC HSP78-GFP	Mat a; his3-Δ200; leu 2-3,112; lys2-801; trp1-1(am); ura3-52; MDM34AAAY-9MYC::KANMX; HSP78-GFP::TRP	This study
821	OM45-GFP rsp5Δ pspt23ΔCT	Mat a; his3-Δ200; leu 2-3,112; lys2-801; trp1-1(am); ura3-52; OM45-GFP::KANMX4; rsp5::HIS3; pSPT23[1-686]-URA3	This study

endonuclease digestions, fill-in reactions with Klenow fragment, and ligations, were performed by standard methods.[60] Deletion strains and strains carrying genes encoding proteins with MYC or GFP tags were constructed by one-step gene replacement, with PCR-generated cassettes.[61,62] We obtained the *mdm30Δ and rsp5Δ* strains carrying tagged ERMES protein genes by adding the tag sequence to the gene concerned in the MHY501 strain, crossing with strains carrying a deletion and then carrying out tetrad dissection and analyzing the haploid Mat a progeny. The PPPY motif (PPPY→AAAY) of MDM34 was mutated by PCR with the MDM34-3A-S3 primer:

5′-TAACTGGAAATGGGGCATGGAGGATAG*Cgccgcagct-tatcat*CGTACGCTGCA GGTCGAC-3′.

The p*MDM12-13MYC* and p*MDM12[3A]-13MYC* plasmids were constructed as follows: the *MDM12-13MYC* coding

Table 2. Plasmids.

No.	Plasmid name	Description	Source/Ref
333	Pø	*TRP1*, 2μ	[64]
350	pUb	*CUP1* promoter, Ub, *TRP*, 2μ	[66]
360	p6His-Ub	*CUP1* promoter, 6His-Ub, *TRP*, 2μ,	[71]
457	pYX142-mtGFP	*TPI* promoter, Mt-GFP, *LEU2*, CEN	[63]
498	Yiplac128-Mito-GFP	*TEF* promoter, Mito-GFP, INT	This study
497	Yiplac128-Mito-mCherry	*TEF* promoter, Mito-mCherry, INT	This study
481	YIPlac204TKC-GFP-HDEL	*TPI* promoter, Kar2Nter (135 pdb)-GFP-HDEL, INT	Adgene/[65]
424	pYX142-mt-RFP	*TPI* promoter, mt-RFP, *LEU2*, CEN	[72]
MC405	Yep96-8His-Ub	*CUP1* promoter, 8His-Ub, *TRP*, 2μ	This study
MC414	Yep96-8His-UbK0	*CUP1* promoter, 8His-UbK0, *TRP*, 2μ	This study
MC415	Yep96-8His-UbK48only	*CUP1* promoter, 8His-UbK48only, *TRP*, 2μ	This study
MC422	Yep96-8His-UbK63only	*CUP1* promoter, 8His-UbK63only, *TRP*, 2μ	This study
MC409	PRS316-*MDM12-13MYC*	*MDM12-13MYC*, *HIS*, CEN	This study
MC410	PRS316-*MDM12[3A]-13MYC*	*MDM12[3PA]-13MYC*, *HIS*, CEN	This study
504	pGFP-ATG8 (416)/GFP-AUT7 (416)	*GFP-ATG8*, *URA3*, CEN	Adgene/[73]
pJMG351	*pMET25-GFP-ATG9*	*MET25-GFP-ATG9*, *URA3*, CEN	[74]

sequence flanked by 1 kb of the promoter region and 0.5 kb of the terminator was amplified by PCR from the genomic DNA of strain *MDM12-13MYC* with primers P324: 5′-agaactagtg-gatcctgttgattgcgacggaagaccagga-3′ and P325: 5′-atcgaattcctg-cagcagttggtagaaaccagcttccat-3′.

The resulting product was inserted into the pRS316 (*URA3*, CEN) plasmid digested with the *Sma*I enzyme with the In-Fusion HD Cloning Kit (Clontech, 638909) to yield p*MDM12-13MYC*.

The p*MDM12-13MYC* plasmid was used as a template for LPSY to AAAY mutagenesis with the QuikChange Lightning Site-Directed Mutagenesis Kit (Agilent Technologies, 210518) Mutagenic primers were designed with the web-based Quik-Change Primer Design Program available online at: www.agilent.com/genomics/qcpd.

The integrative plasmids YIplac128-*MITO-GFP* and YIplac128-*MITO-MCHERRY* were constructed as follows: the mCherry sequence was amplified and used to replace GFP in the pYX232-mtGFP plasmid[63] to yield a pYX232-mtmCherry plasmid. The 2 fusion genes (*MITO-GFP* and *MITO-MCHERRY*) were amplified by PCR and inserted into the p426 plasmid (2μ, URA3) under the control of the TEF promoter and with the CYC1 terminator.[64] The plasmids obtained were then used as a template for amplification of the pTEF-*MITO-GFP*-terCYC and pTEF-*MITO-MCHERRY*-terCYC cassettes with the Yiplac128-TEF-F and CYC-Yiplac128-R primers: (Yiplac128-TEF-F: 5′-TCTAGAGGATCCCCGGGTACCGAG CTCATAGCTTCAAAATGTTTCT-3′ and CYC-Yiplac128-R: 5′-AGTGAATTCGAGCTC GGTACCGGTACCGGCCG CA AATTAAAGCCTT-3′).

The resulting products were verified by DNA sequencing, and inserted into the YIplac128 plasmid (Leu2/INT) digested with *Kpn*I, with the In-Fusion HD Cloning Kit (Clontech, 638909), to yield YIplac128-*MITO-GFP* and YIplac128-*MITO-MCHERRY*. These 2 plasmids were digested with *Eco*RV (restriction site in *LEU2*) and yeast cells were transformed with 0.5 μg of digested DNA, to generate strains in which *MITO-GFP* or *MITO-MCHERRY* was integrated into the *LEU2* locus. Yeast strains with *GFP-HDEL* (ER marker) integrated into the *TRP1* locus were obtained by transformation with 0.5 μg *Eco*RV-linearized Yiplac204/TKC-GFP-HDEL.[65]

The plasmids Yep96-*8HIS-UB*, Yep96-*8HIS-UB-K0*, Yep96-*8HIS-UB-K63only* and Yep96-*8HIS-UB-K48only* were con-structed as follows: the plasmid Yep96-Ub[66] was used as a template for lysine-to-arginine mutagenesis with the Quik-Change Lightning Site-Directed Mutagenesis Kit (Agilent Technologies, 210518). Mutagenic primers were designed with the web-based QuikChange Primer Design Program available online at www.agilent.com/genomics/qcpd. The 8HIS tag was inserted into the resulting plasmid with the Q5® Site-Directed Mutagenesis Kit (New England BioLabs Inc., E0554S). Inser-tion primers were designed with NEBaseChanger™ software, available at: www.NEBaseChanger.neb.com.

Growth conditions

Microbiological techniques, including yeast growth and plas-mid transformation, were performed as described elsewhere.[67] Yeast cells were grown at 24°C or 30°C in rich medium (YP) 1% yeast extract, 2% peptone; supplemented with 2% glucose (YPD); 2% glycerol (YPG); 2% raffinose (YPR); 2% galactose; or 2% lactate. Cells transformed with plasmids were grown in minimal medium (YNB) containing 0.67% yeast nitrogen base without amino acids (Difco, 291940) and supplemented with a 0.1 g/L of each amino acid and nucleic acid base component (Sigma-Aldrich), except those used for selection. The carbon source was 2% glucose or 2% glycerol.

Western blot analysis

Total protein extracts were prepared by the NaOH and tri-chloroacetic acid (TCA) lysis technique.[68] Treatment with gly-cosidase EndoH$_f$ (New England BioLabs Inc., P0703S) was performed as previously described.[69] Proteins were separated by SDS-PAGE and transferred onto nitrocellulose membranes (GE Healthcare, RPN2020D). The primary antibodies used for immunoblotting were monoclonal anti-MYC (clone 9E10), anti-Pgk1 (Abcam, Ab113687), anti-Vma2 (Abcam, Ab113684) and Anti-VDAC1/Porin (Abcam, Ab18988) anti-bodies. The primary antibodies were detected by incubation with horseradish peroxidase (HRP)-conjugated anti-mouse sec-ondary antibodies (Sigma-Aldrich, A9044), followed by ECL

chemiluminescence (Clarity Western ECL Kit, Bio-Rad, 1705060). Unless specified, immunoblotting images were acquired with a Gel Doc̆ XR+ (Bio-Rad) and processed with Image Lab Software. Free GFP was quantified with Image Lab 3.0 build 11 software. For ubiquitin detection, total protein extracts were prepared as described above and separated by SDS-PAGE in 15% Tris-glycine gels. The proteins were transferred to a PVDF (polyvinylidene fluoride) membrane (Merck Millipore, IPVH00010) previously activated by incubation in 100% ethanol for 5 min at room temperature and washed twice in transfer buffer. After transfer, the membrane was boiled in water for 15 min, then saturated with 5% BSA (Sigma-Aldrich, A7906) and incubated with monoclonal anti-ubiquitin antibodies directly coupled to HRP (Enzo Life Sciences, BML-PW0935-0025).

We analyzed protein turnover by adding 100 μg/mL cycloheximide (CHX; Sigma-Aldrich, 7698-1G) to the yeast cultures grown at 24°C, which were then shifted to 37°C. Total protein extracts were prepared at the indicated time points after CHX addition and processed as previously described.

Fluorescence microscopy

Fluorescence microscopy was carried out with a Zeiss Axio Observer Z1 microscope (Carl Zeiss Microscopy GmbH, Germany) with a 63x oil immersion objective. Images were acquired with an SCMOS ORCA FLASH 4.0 charge-coupled device camera (Hamamatsu Photonics, Japan). Images were acquired with Zen 2012 Package Acquisition/Analyze software and processed with Zen 2012, ImageJ, Photoshop CS5 and Illustrator CS5.

Abbreviations

αF	α factor
AIM	Atg8-interacting motif
CHX	cycloheximide
DIC	differential interference contrast
DRPs	dynamin-related proteins
DUB	deubiquitinating enzyme
ER	endoplasmic reticulum
ERMD	ER-associated mitochondrial division
ERMES	endoplasmic reticulum-mitochondrial encounter structure
HECT	homologous to E6-associated protein C terminus
mtDNA	mitochondrial DNA
NEDD4	neural precursor cell-expressed, developmentally downregulated
Pgk1	phosphoglycerate kinase
Rapa	rapamycin
RBR	RING between RINGs
RING	really interesting new genes
SAM	sorting and assembly machinery
SCF	Skp1/Cullin/F-box protein
SMP	synaptotagmin-like, mitochondrial and lipid-binding proteins
Ub	ubiquitin

References

[1] Westermann B. Mitochondrial fusion and fission in cell life and death. Nat Rev Mol Cell Biol 2010; 11:872-84; PMID:21102612; http://dx.doi.org/10.1038/nrm3013

[2] Mishra P, Chan DC. Mitochondrial dynamics and inheritance during cell division, development and disease. Nat Rev Mol Cell Biol 2014; 15:634-46; PMID:25237825; http://dx.doi.org/10.1038/nrm3877

[3] Friedman JR, Nunnari J. Mitochondrial form and function. Nature 2014; 505:335-43; PMID:24429632; http://dx.doi.org/10.1038/nature12985

[4] Friedman JR, Lackner LL, West M, Dibenedetto JR, Nunnari J, Voeltz GK. ER Tubules mark sites of mitochondrial division. Science 2011; 334:358-62; PMID:21885730; http://dx.doi.org/10.1126/science.1207385

[5] Klecker T, Böckler S, Westermann B. Making connections: interorganelle contacts orchestrate mitochondrial behavior. Trends Cell Biol 2014:1-9

[6] Stroud DA, Oeljeklaus S, Wiese S, Bohnert M, Lewandrowski U, Sickmann A, Guiard B, van der Laan M, Warscheid B, Wiedemann N. Composition and topology of the endoplasmic reticulum-mitochondria encounter structure. J Mol Biol 2011; 413:743-50; PMID:21945531; http://dx.doi.org/10.1016/j.jmb.2011.09.012

[7] Kornmann B, Osman C, Walter P. The conserved GTPase Gem1 regulates endoplasmic reticulum-mitochondria connections. Proc Natl Acad Sci USA 2011; 108:14151-6; PMID:21825164; http://dx.doi.org/10.1073/pnas.1111314108

[8] Hobbs AE, Srinivasan M, McCaffery JM, Jensen RE. Mmm1p, a mitochondrial outer membrane protein, is connected to mitochondrial DNA (mtDNA) nucleoids and required for mtDNA stability. J Cell Biol 2001; 152:401-10; PMID:11266455; http://dx.doi.org/10.1083/jcb.152.2.401

[9] Meeusen S, Nunnari J. Evidence for a two membrane-spanning autonomous mitochondrial DNA replisome. J Cell Biol 2003; 163:503-10; PMID:14597773; http://dx.doi.org/10.1083/jcb.200304040

[10] Murley A, Lackner LL, Osman C, West M, Voeltz GK, Walter P, Nunnari J. ER-associated mitochondrial division links the distribution of mitochondria and mitochondrial DNA in yeast. eLife 2013; 2: e00422; PMID:23682313; http://dx.doi.org/10.7554/eLife.00422

[11] Meisinger C, Rissler M, Chacinska A, Szklarz LKS, Milenkovic D, Kozjak V, Schönfisch B, Lohaus C, Meyer HE, Yaffe MP, et al. The mitochondrial morphology protein Mdm10 functions in assembly of the preprotein translocase of the outer membrane. Dev Cell 2004; 7:61-71; PMID:15239954; http://dx.doi.org/10.1016/j.devcel.2004.06.003

[12] Mao K, Wang K, Liu X, Klionsky DJ. The scaffold protein Atg11 recruits fission machinery to drive selective mitochondria degradation by autophagy. Dev Cell 2013; 26:9-18; PMID:23810512; http://dx.doi.org/10.1016/j.devcel.2013.05.024

[13] Mao K, Klionsky DJ. Participation of mitochondrial fission during mitophagy. Cell Cycle 2013; 12:0-1; http://dx.doi.org/10.4161/cc.26352

[14] Böckler S, Westermann B. Mitochondrial ER contacts are crucial for mitophagy in yeast. Dev Cell 2014; 28:450-8; PMID:24530295; http://dx.doi.org/10.1016/j.devcel.2014.01.012

[15] Kopec KO, Alva V, Lupas AN. Homology of SMP domains to the TULIP superfamily of lipid-binding proteins provides a structural basis for lipid exchange between ER and mitochondria. Bioinformatics 2010; 26:1927-31; PMID:20554689; http://dx.doi.org/10.1093/bioinformatics/btq326

[16] Lang A, John Peter AT, Kornmann B. ER-mitochondria contact sites in yeast: beyond the myths of ERMES. Curr Opin Cell Biol 2015; 35:7-12; PMID:25836730; http://dx.doi.org/10.1016/j.ceb.2015.03.002

[17] AhYoung AP, Jiang J, Zhang J, Khoi Dang X, Loo JA, Zhou ZH, Egea PF. Conserved SMP domains of the ERMES complex bind phospholipids and mediate tether assembly. Proc Natl Acad Sci USA 2015; 112:E3179-88; PMID:26056272; http://dx.doi.org/10.1073/pnas.1422363112

[18] Cohen Y, Klug YA, Dimitrov L, Erez Z, Chuartzman SG, Elinger D, Yofe I, Soliman K, Gärtner J, Thoms S, et al. Peroxisomes are juxtaposed to strategic sites on mitochondria. Mol Biosyst 2014; 10:1742-8; PMID:24722918; http://dx.doi.org/10.1039/C4MB00001C

[19] Ušaj MM, Brložnik M, Kaferle P, Žitnik M, Wolinski H, Leitner F, Kohlwein SD, Zupan B, Petrovič U. Genome-wide localization study of yeast Pex11 identifies peroxisome-mitochondria interactions through the ERMES complex. J Mol Biol 2015; 427(11):2072-87:1-16

[20] Ota K, Kito K, Okada S, Ito T. A proteomic screen reveals the mitochondrial outer membrane protein Mdm34p as an essential target of the F-box protein Mdm30p. Genes Cells 2008; 13:1075-85; http://dx.doi.org/10.1111/j.1365-2443.2008.01228.x

[21] Komander D, Rape M. The ubiquitin code. Annu Rev Biochem 2012; 81:203-29; PMID:22524316; http://dx.doi.org/10.1146/annurev-biochem-060310-170328

[22] Rotin D, Kumar S. Physiological functions of the HECT family of ubiquitin ligases. Nat Rev Mol Cell Biol 2009; 10:398-409; PMID:19436320; http://dx.doi.org/10.1038/nrm2690

[23] Smit JJ, Sixma TK. RBR E3-ligases at work. EMBO Rep 2014; 15:142-54; PMID:24469331; http://dx.doi.org/10.1002/embr.201338166

[24] Zoladek T, Tobiasz A, Vaduva G, Boguta M, Martin NC, Hopper AK. MDP1, a Saccharomyces cerevisiae gene involved in mitochondrial/cytoplasmic protein distribution, is identical to the ubiquitin-protein ligase gene RSP5. Genetics 1997; 145:595-603; PMID:9055070

[25] Fisk HA, Yaffe MP. A role for ubiquitination in mitochondrial inheritance in Saccharomyces cerevisiae. J Cell Biol 1999; 145:1199-208; PMID:10366593; http://dx.doi.org/10.1083/jcb.145.6.1199

[26] Fritz S, Weinbach N, Westermann B. Mdm30 is an F-box protein required for maintenance of fusion-competent mitochondria in yeast. Mol Biol Cell 2003; 14:2303-13; PMID:12808031; http://dx.doi.org/10.1091/mbc.E02-12-0831

[27] Cohen MMJ, Leboucher GP, Livnat-Levanon N, Glickman MH, Weissman AM. Ubiquitin-proteasome-dependent degradation of a mitofusin, a critical regulator of mitochondrial fusion. Mol Biol Cell 2008; 19:2457-64; PMID:18353967; http://dx.doi.org/10.1091/mbc.E08-02-0227

[28] Youle RJ, Narendra DP. Mechanisms of mitophagy. Nat Rev Mol Cell Biol 2011; 12:9-14; PMID:21179058; http://dx.doi.org/10.1038/nrm3028

[29] Birgisdottir AB, Lamark T, Johansen T. The LIR motif - crucial for selective autophagy. J Cell Sci 2013; 126:3237-47; PMID:23908376

[30] Okamoto K, Kondo-Okamoto N, Ohsumi Y. Mitochondria-anchored receptor Atg32 mediates degradation of mitochondria via selective autophagy. Dev Cell 2009; 17:87-97; PMID:19619494; http://dx.doi.org/10.1016/j.devcel.2009.06.013

[31] Kanki T, Wang K, Cao Y, Baba M, Klionsky DJ. Atg32 Is a Mitochondrial Protein that confers selectivity during mitophagy. Dev Cell 2009; 17:98-109; PMID:19619495; http://dx.doi.org/10.1016/j.devcel.2009.06.014

[32] Byrd RA, Weissman AM. Compact Parkin only: insights into the structure of an autoinhibited ubiquitin ligase. EMBO J 2013; 32:2087-9; PMID:23852447; http://dx.doi.org/10.1038/emboj.2013.158

[33] Narendra D, Tanaka A, Suen DF, Youle RJ. Parkin is recruited selectively to impaired mitochondria and promotes their autophagy. J Cell Biol 2008; 183:795-803; PMID:19029340; http://dx.doi.org/10.1083/jcb.200809125

[34] Müller M, Kötter P, Behrendt C, Walter E, Scheckhuber CQ, Entian KD, Reichert AS. Synthetic quantitative array technology identifies the Ubp3-Bre5 deubiquitinase complex as a negative regulator of mitophagy. Cell Reports 2015; 10:1215-25; PMID:25704822; http://dx.doi.org/10.1016/j.celrep.2015.01.044

[35] Hesselberth JR, Miller JP, Golob A, Stajich JE, Michaud GA, Fields S. Comparative analysis of Saccharomyces cerevisiae WW domains and their interacting proteins. Genome Biol 2006; 7:R30; PMID:16606443; http://dx.doi.org/10.1186/gb-2006-7-4-r30

[36] Gupta R, Kus B, Fladd C, Wasmuth J, Tonikian R, Sidhu S, Krogan NJ, Parkinson J, Rotin D. Ubiquitination screen using protein microarrays for comprehensive identification of Rsp5 substrates in yeast. Mol Syst Biol 2007; 3:116; PMID:17551511; http://dx.doi.org/10.1038/msb4100159

[37] Hoppe T, Matuschewski K, Rape M, Schlenker S, Ulrich HD, Jentsch S. Activation of a membrane-bound transcription factor by regulated ubiquitin/proteasome-dependent processing. Cell 2000; 102:577-86; PMID:11007476; http://dx.doi.org/10.1016/S0092-8674(00)00080-5

[38] Kamińska J, Kwapisz M, Grabińska K, Orłowski J, Boguta M, Palamarczyk G, Żołądek T. Rsp5 ubiquitin ligase affects isoprenoid pathway and cell wall organization in S. cerevisiae. Acta biochim Pol 2005; 52:207-20; PMID:15827618

[39] Belgareh-Touzé N, Léon S, Erpapazoglou Z, Stawiecka-Mirota M, Urban-Grimal D, Haguenauer-Tsapis R. Versatile role of the yeast ubiquitin ligase Rsp5p in intracellular trafficking. Biochem Soc Trans 2008; 36:791-6; http://dx.doi.org/10.1042/BST0360791

[40] Neutzner A, Youle RJ. Instability of the mitofusin Fzo1 regulates mitochondrial morphology during the mating response of the yeast Saccharomyces cerevisiae. J Biol Chem 2005; 280:18598-603; PMID:15760898; http://dx.doi.org/10.1074/jbc.M500807200

[41] Thrower JS, Hoffman L, Rechsteiner M, Pickart CM. Recognition of the polyubiquitin proteolytic signal. EMBO J 2000; 19:94-102; PMID:10619848; http://dx.doi.org/10.1093/emboj/19.1.94

[42] Burgess SM, Delannoy M, Jensen RE. MMM1 encodes a mitochondrial outer membrane protein essential for establishing and maintaining the structure of yeast mitochondria. J Cell Biol 1994; 126:1375-91; PMID:8089172; http://dx.doi.org/10.1083/jcb.126.6.1375

[43] Dimmer KS, Fritz S, Fuchs F, Messerschmitt M, Weinbach N, Neupert W, Westermann B. Genetic basis of mitochondrial function and morphology in Saccharomyces cerevisiae. Mol Biol Cell 2002; 13:847-53; PMID:11907266; http://dx.doi.org/10.1091/mbc.01-12-0588

[44] Sogo LF, Yaffe MP. Regulation of mitochondrial morphology and inheritance by Mdm10p, a protein of the mitochondrial outer membrane. J Cell Biol 1994; 126:1361-73; PMID:8089171; http://dx.doi.org/10.1083/jcb.126.6.1361

[45] Berger KH, Sogo LF, Yaffe MP. Mdm12p, a component required for mitochondrial inheritance that is conserved between budding and fission yeast. J Cell Biol 1997; 136:545-53; PMID:9024686; http://dx.doi.org/10.1083/jcb.136.3.545

[46] Cebollero E, Reggiori F. Regulation of autophagy in yeast Saccharomyces cerevisiae. Biochim Biophys Acta 2009; 1793:1413-21; PMID:19344676; http://dx.doi.org/10.1016/j.bbamcr.2009.01.008

[47] Kissova I, Deffieu M, Manon S, Camougrand N. Uth1p is involved in the autophagic degradation of mitochondria. J Biol Chem 2004; 279:39068-74; PMID:15247238; http://dx.doi.org/10.1074/jbc.M406960200

[48] Tal R, Winter G, Ecker N, Klionsky DJ, Abeliovich H. Aup1p, a yeast mitochondrial protein phosphatase homolog, is required for efficient

stationary phase mitophagy and cell survival. J Biol Chem 2007; 282:5617-24; PMID:17166847; http://dx.doi.org/10.1074/jbc.M6059 40200

[49] Klionsky DJ, Abdalla FC, Abeliovich H, Abraham RT, Acevedo-Arozena A, Adeli K, Adeli K, Agholme L, Agnello M, Agostinis P, et al. Guidelines for the use and interpretation of assays for monitoring autophagy. Autophagy 2012; 8:445-544; PMID:22966490; http://dx. doi.org/10.4161/auto.19496

[50] Rosado CJ, Mijaljica D, Hatzinisiriou I, Prescott M, Devenish RJ. Rosella: a fluorescent pH-biosensor for reporting vacuolar turnover of cytosol and organelles in yeast. Autophagy 2008; 4:205-13; PMID:18094608; http://dx.doi.org/10.4161/auto.5331

[51] Abeliovich H, Zarei M, Rigbolt KT, Youle RJ, Dengjel J. Involvement of mitochondrial dynamics in the segregation of mitochondrial matrix proteins during stationary phase mitophagy. Nat Commun 2013; 4:2789; PMID:24240771; http://dx.doi.org/10.1038/ncomms3789

[52] Lynch-Day MA, Klionsky DJ. The Cvt pathway as a model for selective autophagy. FEBS Lett 2010; 584:1359-66; PMID:20146925; http://dx.doi.org/10.1016/j.febslet.2010.02.013

[53] Lu K, Psakhye I, Jentsch S. Autophagic clearance of PolyQ proteins mediated by Ubiquitin-Atg8 adaptors of the conserved CUET protein family. Cell 2014; 158:549-63; PMID:25042851; http://dx.doi.org/10.1016/j.cell.2014.05.048

[54] Mari M, Reggiori F. Atg9 trafficking in the yeast *Saccharomyces cerevisiae*. Autophagy 2007; 3:145-8; PMID:17204846; http://dx.doi.org/10.4161/auto.3608

[55] Wu X, Li L, Jiang H. Doa1 targets ubiquitinated substrates for mitochondria-associated degradation. J Cell Biol 2016; 213:49-63; PMID:27044889; http://dx.doi.org/10.1083/jcb.201510098

[56] Kee Y, Lyon N, Huibregtse JM. The Rsp5 ubiquitin ligase is coupled to and antagonized by the Ubp2 deubiquitinating enzyme. EMBO J 2005; 24:2414-24; PMID:15933713; http://dx.doi.org/10.1038/sj.emboj.7600710

[57] Ossareh-Nazari B, Cohen M, Dargemont C. The Rsp5 ubiquitin ligase and the AAA-ATPase Cdc48 control the ubiquitin-mediated degradation of the COPII component Sec23. Exp Cell Res 2010; 316:3351-7; PMID:20846524; http://dx.doi.org/10.1016/j.yexcr.2010.09.005

[58] Baxter BK, Abeliovich H, Zhang X, Stirling AG, Burlingame AL, Goldfarb DS. Atg19p ubiquitination and the cytoplasm to vacuole trafficking pathway in yeast. J Biol Chem 2005; 280:39067-76; PMID:16186126; http://dx.doi.org/10.1074/jbc.M508064200

[59] Finley D, Ozkaynak E, Varshavsky A. The yeast polyubiquitin gene is essential for resistance to high temperatures, starvation, and other stresses. Cell 1987; 48:1035-46; PMID:3030556; http://dx.doi.org/10.1016/0092-8674(87)90711-2

[60] Maniatis T, Fritsch ET, Sambrook J. Molecular Cloning: A Laboratory Manual. Cold Spring Harbor, NY: Cold Spring Harbor Laboratory Press 1982

[61] Janke C, Magiera MM, Rathfelder N, Taxis C, Reber S, Maekawa H, Moreno-Borchart A, Doenges G, Schwob E, Schiebel E, et al. A versatile toolbox for PCR-based tagging of yeast genes: new fluorescent proteins, more markers and promoter substitution cassettes. Yeast 2004; 21:947-62; PMID:15334558; http://dx.doi.org/10.1002/yea.1142

[62] Longtine MS, McKenzie A, Demarini DJ, Shah NG, Wach A, Brachat A, Philippsen P, Pringle JR. Additional modules for versatile and economical PCR-based gene deletion and modification in *Saccharomyces cerevisiae*. Yeast 1998; 14:953-61; PMID:9717241; http://dx.doi.org/10.1002/(SICI)1097-0061(199807)14:10%3c953::AID-YEA293%3e3.0.CO;2-U

[63] Westermann B, Neupert W. Mitochondria-targeted green fluorescent proteins: convenient tools for the study of organelle biogenesis in *Saccharomyces cerevisiae*. Yeast 2000; 16:1421-7; PMID:11054823; http://dx.doi.org/10.1002/1097-0061(200011)16:15%3c1421::AID-YEA624%3e3.0.CO;2-U

[64] Mumberg D, Müller R, Funk M. Yeast vectors for the controlled expression of heterologous proteins in different genetic backgrounds. Gene 1995; 156:119-22; PMID:7737504; http://dx.doi.org/10.1016/0378-1119(95)00037-7

[65] Rossanese OW, Reinke CA, Bevis BJ, Hammond AT, Sears IB, O'Connor J, Glick BS. A role for actin, Cdc1p, and Myo2p in the inheritance of late Golgi elements in *Saccharomyces cerevisiae*. J Cell Biol 2001; 153:47-62; PMID:11285273; http://dx.doi.org/10.1083/jcb.153.1.47

[66] Ecker DJ, Khan MI, Marsh J, Butt TR, Crooke ST. Chemical synthesis and expression of a cassette adapted ubiquitin gene. J Biol Chem 1987; 262:3524-7; PMID:3029116

[67] Rickwood DD, B, Darley-Usmar VM. Yeast Mitochondria. Campbell I, Duffus JH, ed. Yeast- a practical approach: Oxford: IRL Press Limited, 1988; 185.

[68] Volland C, Urban-Grimal D, Géraud G, Haguenauer-Tsapis R. Endocytosis and degradation of the yeast uracil permease under adverse conditions. J Biol Chem 1994; 269:9833-41; PMID:8144575

[69] Kornmann B, Currie E, Collins SR, Schuldiner M, Nunnari J, Weissman JS, Walter P. An ER-mitochondria tethering complex revealed by a synthetic biology screen. Science 2009; 325:477-81; PMID:19556461; http://dx.doi.org/10.1126/science.1175088

[70] Swanson R, Locher M, Hochstrasser M. A conserved ubiquitin ligase of the nuclear envelope/endoplasmic reticulum that functions in both ER-associated and Matalpha2 repressor degradation. Genes Dev 2001; 15:2660-74; PMID:11641273; http://dx.doi.org/10.1101/gad.933301

[71] Morvan J, Froissard M, Haguenauer-Tsapis R, Urban-Grimal D. The ubiquitin ligase Rsp5p is required for modification and sorting of membrane proteins into multivesicular bodies. Traffic 2004; 5:383-92; PMID:15086787; http://dx.doi.org/10.1111/j.1398-9219.2004.00183.x

[72] Thiaville PC, El Yacoubi B, Perrochia L, Hecker A, Prigent M, Thiaville JJ, Forterre P, Namy O, Basta T, de Crécy-Lagard V. Cross kingdom functional conservation of the core universally conserved threonylcarbamoyladenosine tRNA synthesis enzymes. Eukaryot Cell 2014; 13:1222-31; PMID:25038083; http://dx.doi.org/10.1128/EC.00147-14

[73] Guan J, Stromhaug PE, George MD, Habibzadegah-Tari P, Bevan A, Dunn WA, Jr, Klionsky DJ. Cvt18/Gsa12 is required for cytoplasm-to-vacuole transport, pexophagy, and autophagy in *Saccharomyces cerevisiae* and *Pichia pastoris*. Mol Biol Cell 2001; 12:3821-38; PMID:11739783; http://dx.doi.org/10.1091/mbc.12.12.3821

[74] Bugnicourt A, Mari M, Reggiori F, Haguenauer-Tsapis R, Galan JM. Irs4p and Tax4p: two redundant EH domain proteins involved in autophagy. Traffic 2008; 9:755-69; PMID:18298591; http://dx.doi.org/10.1111/j.1600-0854.2008.00715.x